TNO-report TNO-MEP – R 96/406

TNO Institute of Environmental Sciences, Energy Research and Process Innovation Effects of clouds, stratospheric ozone depletion and tropospheric pollution on the chemical budget of ozone in the troposphere through changes in photolysis rates

Laan van Westenenk 501 P.O. Box 342 7300 AH Apeldoorn The Netherlands

Phone +31 55 - 549 34 93 Fax +31 55 - 541 98 37 Date
December 1996

Author(s)
Jianzhong Ma

with cooperation of:
Michiel van Weele (IMAU)
Robert Guicherit
Michiel Roemer

Order no. 53398

Keywords

- photolysis rate change
- tropospheric ozone

Intended for

All rights reserved.

No part of this publication may be reproduced and/or published by print, photoprint, microfilm or any other means without the previous written consent of TNO.

In case this report was drafted on instructions, the rights and obligations of contracting parties are subject to either the Standard Conditions for Research Instructions given to TNO, or the relevant agreement concluded between the contracting parties. Submitting the report for inspection to parties who have a direct interest is permitted.

© 1996 TNO

The Quality System of the TNO Institute of Environmental Sciences, Energy Research and Process Innovation has been certified in accordance with ISO 9001.

The TNO Institute of Environmental Sciences, Energy Research and Process Innovation is a recognized contract research institute for industry and government with expertise in sustainable development and environmentally oriented process innovation.

Netherlands Organization for Applied Scientific Research TNO

The Standard Conditions for research instructions given to TNO, as filed at the Registry of the District Court and the Chamber of Commerce in The Hague shall apply to all instructions given to TNO.

TNO-MEP - R 96/406 3 of 69th

Abstract

The extended PHATIMA has been used to study the effects of clouds, stratospheric ozone depletion, and tropospheric pollution on the chemical budget of tropospheric ozone at the mid-latitudes of the Northern Hemisphere through the changes in photolysis rates. The changes in the rates of the net production of ozone with these radiation perturbations, have been shown for each altitude over the ocean, clean continent and polluted continent, and also for column integration of the planetary boundary layer and the free troposphere as well the total troposphere. The changes in photodissociation coefficients and chemical reactions that are most important for the chemical budget of tropospheric ozone have been discussed. In addition to NO_x, the water vapor has been shown to play an important role as well in determining the ozone budget in the troposphere. The response of the net production of ozone with stratospheric ozone depletion in the polluted boundary layer has been addressed by considering various conditions of NO_x and NMHC_s. It has been shown that the response is not only determined dominately by the NO_x, but also affected secondly by the NMHC_s, with the increase in the net production of ozone being more favored in the NMHC_s limited region than in the NO_x limited region.

Contents

Abstract	3		
1.	Introduction		
2.	Photochemistry		
3.	Model Description173.1 Radiation Model173.2 Extended PHATIMA18		
4.	Results and Discussion 23 4.1 J_values 23 4.1.1 Effect of clouds 23 4.1.2 Effect of stratospheric ozone depletion 25 4.1.3 Effect of tropospheric pollution 28 4.2 Net Ozone Production 28 4.2.1 Effect of clouds 29 4.2.2 Effect of stratospheric ozone depletion 34 4.2.3 Effect of tropospheric pollution 42 4.3 Chemical Reactions 43 4.3.1 Effect of clouds 45 4.3.2 Effect of stratospheric ozone depletion 51 4.3.3 Effect of tropospheric pollution 60		
5.	Conclusions61		
6.	References		
7.	Authentication 69		

TNO-MEP - R 96/406 7 of 69th

1. Introduction

Tropospheric ozone (O₃) is an important trace gas in the atmosphere. Radiatively, ozone acts as a greenhouse gas itself, since it can absorb terrestrial infrared radiation and hence cause a warming of the atmosphere [Fishman et al., 1979; Ramanathan et al., 1987; Lacis et al., 1990; Roemer, 1991; Lelieveld and Van Dorland; 1995]. Chemically, ozone is the primary source of hydroxyl radicals (OH) [Levy, 1971], which are responsible for the oxidation removal of many trace gases, such as methane (CH4), hydrofluorocarbons (HFCs), hydrochloro fluorocarbons (HCFCs), that influence climate and/or are important for the stratospheric ozone layer [Weinstock and Niki, 1972; Wofsy et al., 1972; WMO, 1990]. Tropospheric ozone arises from two processes: downward flux from the stratosphere; and in situ photochemical production from the oxidation of hydrocarbons and carbon monoxide (CO) in the presence of nitrogen oxides (NO_x=NO+NO₂, with NO=nitric oxide and NO₂=nitrogen dioxide) [Junge, 1962; Chamedies and Walker, 1973; Crutzen, 1974; Liu et al., 1980]. Ozone is removed from the troposphere by in situ chemistry and by uptake at the Earth's surface.

There is some evidence to suggest that ozone concentrations in the troposphere of the Northern Hemisphere have increased by a factor of two or more over the past 100 years, with most of the increase having occurred since 1950. During the same time, a statistically negative trend of 0.5% yr⁻¹ is observed at the South Pole [IPPC, 1990; WMO, 1992 & 1995]. The increased emissions of precursors, e.g., NO_x, CO, and hydrocarbons, by human activities, such as fossil fuel burning in industrial areas and biomass burning in South America and Africa, lead to enhanced photochemical production of ozone in the troposphere [WMO, 1995]. While the surface ozone decrease observed at the South Pole can be related to the higher levels of methane and carbon monoxide due to the enhanced biological activities in the ocean at that season, it may also be due to the extreme conditions of UV increase experienced under the Antarctic ozone hole [Schnell et al., 1991]. The Antarctic ozone hole and global stratospheric ozone depletion have now been unequivocally related to anthropogenic emissions of chlorofluorocarbons (CFCs) [WMO, 1992].

Due to the large number of processes that control tropospheric ozone, numeric models have been extensively used in studies of the budget and distribution of ozone in the troposphere. To cover various spatial and temporal scales with limited computer resources, different types of models have been used for the specific purpose [WMO, 1995]. Box (0-dimensional) and one-dimensional models have been used, commonly in earlier studies, to estimate the chemical budget of tropospheric ozone. For example, Liu et al. [1980] investigated the effects of NO_x intrusion from the stratosphere, as well as NO_x emissions from high flying subsonic aircraft in the northern hemisphere, on photochemical ozone production in the upper troposphere by a diurnal one-dimensional photochemical calculation. With a box model, Liu et al. [1987] and Lin et al. [1988] studied the non-linear relationship between the

ozone production and the concentrations of its precursors, and showed that the O₃ production per unit of NO_x is greater for lower NO_x. By using their box model [Liu et al, 1987 and Lin et al. 1988], Liu and Trainer [1988] studied the response of the tropospheric ozone and odd hydrogen radicals to column ozone change, and showed that the response depends critically on the local NO_x concentration. Liu [1988] also estimated the net ozone production in various regions characterized by the NO_x distribution, such as industrial areas, biomass burning area, free troposphere, and remote boundary layers. Thompson [1984] studied the effect of clouds on photolysis rates and ozone formation in the marine troposphere by using an one-dimensional photochemical transport model. The modified version of this model [Thompson and Cicerone, 1982 & 1986] was also used to evaluate the effect of convective clouds on tropospheric ozone production with modelling and analysis of field data [Pickering et al., 1990]. Different box models were still used recently by Davis et al. (1996) for the assessment of ozone photochemistry with observations in the western North Pacific.

Two-dimensional models have been widely used for several years to study tropospheric ozone on a global scale [e.g., Roemer and van der Hout, 1992; Law and Pyle, 1993; Strand and Hov, 1994; Roemer, 1995; WMO, 1995]. With theses models, a coarse global distribution pattern of tropospheric ozone is shown, and a wide range of studies, such as the long-term trend of ozone among other important species in the troposphere, have been carried out. A limitation of two-dimensional models is that they are unable to resolve longitudinal variations in several species that are important for the ozone chemistry, in particular in NO_x mixing ratios, between different regions. The zonal averaging approach in two-dimensional models tends to overestimate the ozone and hydroradical concentrations [Liu, et al., 1987; Lin et al., 1988; Kanakidou and Crutzen, 1993; Matthijsen, 1995].

Three-dimensional models have been increasingly used to study the budget of tropospheric ozone on the global and continental scales [WMO, 1995]. The budget of ozone over the North American continent in summer was examined recently using the results of a three-dimensional model simulation [Jacob et al., 1993a, 1993b; Chin et al., 1994]. Jacob et al. [1993b] estimated that export of U.S. pollution supplies 35 Tg ozone to the global troposphere in summer (90 days), half of which is produced downwind of the U.S., following export of NO_x. The ozone model of EMEP MSC-W (European Monitoring and Evaluation Programme, Meteorological Synthesizing Centre-West) has been used to study photochemistry over Europe for two extended summer periods in 1985 and 1989 [Simpson, 1993]. The study showed that NO_x limits ozone formation in the European boundary layer in most locations, whereas NMHCs limit the production mostly in polluted areas. The three-dimensional Eulerian model of LOTOS (LOng Term Ozone Simulation) has been used to calculate the ozone budget over the entire European area and in the lowest 2.5 km of the troposphere for the year 1991 [Roemer et al., 1995]. The results indicated that there is a net chemical production of about 21 Tg ozone per month in the summer(July-August), and a net transport, out of Europe, of about 4

TNO-MEP - R 96/406 9 of 69th

Tg/month. The effect of cloud convection on the ozone budget of the troposphere has been addressed with both global [Lelieveld and Crutzen, 1994] and regional [Flatφy et al., 1995] three-dimensional models. The results showed that the physical processes, especially convection, can play an important role in the distribution and budget of tropospheric ozone. Several attempts have been made to study the global distribution and budget of ozone in the troposphere by using the three-dimensional global-scale chemical transport models [e.g., Müller and Brasseur, 1995; Roelofs and Lelieveld, 1995]. The modeled global distribution and budget of tropospheric ozone are generally in good agreement with observations, even though there are still some deficiencies to be improved.

In this paper, the extended version of an one-dimensional model, PHATIMA (PHotochemistry And Transport In Mid-latitude Atmosphere), is used to study the effects of clouds, stratospheric ozone depletions and tropospheric pollutants, through changes in photolysis rates, on the net chemical production of ozone in the troposphere. The model simulations are performed for the summer-time in the mid-latitude of the Northern Hemisphere, with various regions including ocean, clean continent and polluted continent. In section 2, the chemical reactions concerning the chemical budget of ozone in the troposphere are described. In section 3, the radiative transfer model used to calculate photolysis rates and the extended PHATIMA are briefly introduced. In section 4, the results provided by the model are presented and discussed. Conclusions are given in section 5.

TNO-MEP - R 96/406 11 of 69th

2. Photochemistry

Photodissociation of O_3 in the troposphere yielding $O(^1D)$,

$$O_3 + hv(\lambda < 320 \text{ nm}) \rightarrow O(^1D) + O_2 \tag{R1}$$

followed by

$$O(^{1}D) + H_{2}O \rightarrow 2OH \tag{R2}$$

acts initially as a sink for O_3 , and the main source of OH radicals. The $O(^1D)$ radical does not necessarily react with water vapor, but more likely with molecular oxygen or nitrogen,

$$O(^{1}D) + M(N_{2}; O_{2}) \rightarrow O(^{3}P) + M$$
 (R3)

By reaction (R3), the $O(^1D)$ radical is deactivated. The ground-state $O(^3P)$ reacts mainly with molecular oxygen forming ozone again (via R7). Therefore, the reaction of the $O(^1D)$ atom with water vapor, (R2), is the rate-determining step in the loss of tropospheric ozone through the photolysis of O_3 itself. Additional losses occur through the reaction of the HO_2 radical with O_3 via (R4) and (to a smaller extent) through the reaction of OH with O_3 (R5), i.e., the HO_x (= OH + HO_2) catalytic cycle.

$$HO_2 + O_3 \rightarrow OH + 2O_2 \tag{R4}$$

$$HO + O_3 \rightarrow HO_2 + O_2$$
 (R5)

Formation of ozone in the troposphere is accomplished by the photolysis of NO₂, (R6), followed by the reaction of the formed O(³P) radical with molecular oxygen, (R7).

$$NO_2 + h\nu(\lambda < 420 \text{ nm}) \rightarrow NO + O(^3P)$$
 (R6)

$$O(^3P) + O_2 + M \rightarrow O_3 + M \tag{R7}$$

This ozone formation is strong limited since the NO produced in the same reaction reacts rapidly with O₃, which yields NO₂ again, (R8).

$$NO + O_3 \rightarrow NO_2 + O_2 \tag{R8}$$

However, peroxy radicals (HO₂ and CH₃O₂, etc.), formed in the oxidation of CO and hydrocarbons by OH, can convert NO back to NO₂ in competition with (R8). The oxidation of CO to generate ozone is via (R9), (R10) and (R11) followed by (R6) and (R7).

$$CO + OH \rightarrow CO_2 + H$$
 (R9)

$$H + O_2 + M \rightarrow HO_2 + M \tag{R10}$$

$$HO_2 + NO \rightarrow OH + NO_2$$
 (R11)

Typical mechanism for the oxidation of hydrocarbons are as the following

$$RH + OH \rightarrow R + H_2O \tag{R12}$$

$$R + O_2 + M \to RO_2 + M \tag{R13}$$

$$RO_2 + NO \rightarrow RO + NO_2$$
 (R14a)

$$RO + O_2 \rightarrow HO_2 + Carb$$
 (R15)

In addition to RO₂, an initial reaction between a hydrocarbon (RH) and a hydroxyl radical (OH) also leads to the formation of a hydroperoxyl radical (HO₂) and a carbonyl (Carb). Both RO₂ and HO₂ can convert NO back to NO₂ via (R14a) and (R11), respectively, and thus result in the production of ozone through (R6) and (R7). Additional ozone can then be produced from the degration of Carb, in abbreviation, by reaction with OH, (R16), or by photodissociation, (R17).

$$Carb + OH \rightarrow R'O_2 + products$$
 (R16)

$$Carb + hv \rightarrow R'O_2 + HO_2 + products$$
 (R17a)

$$Carb + hv \rightarrow stable \ products$$
 (R17b)

Reaction (R16) represents an OH to HO_2 conversion similar to (R12) followed by reactions (R13) through (R15). However, the photolysis channel (R17a) is a free radical source and, thereby, produces an amplification of the photochemical reactivity.

TNO-MEP - R 96/406 13 of 69th

Hydrocarbons and CO provide the fuel for the production of tropospheric ozone and are consumed in the process. In remote areas, CO and methane (CH4) typically provide the fuel for ozone production. In the urban locations, non-methane hydrocarbons (NMHC_s) are usually the dominant fuel [WMO, 1995 and reference therein]. In contrast to CO and hydrocarbons, NO_x is conserved in the process of ozone production and thus acts as a catalyst in ozone formation. The conversion of NO to NO_2 by peroxyl radicals via (R11) and (R14a) is the crucial step, since the photolysis of NO_2 , (R6), and the reaction followed to produce ozone, (R7), are so fast.

With the consumption of CO and hydrocarbons, ozone is not always net produced since the hydroperoxyl radials, e.g., HO_2 formed in the oxidation, can react with O_3 via (R4) in competition with (R11), and thus leads to the destruction of ozone when the concentration of NO_x is very small. The latter often occurs in the remote oceanic areas where the level of NO_x is normally less than 20 pptv.

The effectiveness of the oxidation of CO and hydrocarbons can be greatly reduced by termination reactions in which two radicals are lost,

$$HO_2 + HO_2 \rightarrow H_2O_2 + O_2 \tag{R18}$$

$$OH + HO_2 \rightarrow H_2O + O_2 \tag{R19}$$

$$OH + OH + M \rightarrow H_2O_2 + M \tag{R20}$$

$$RO_2 + HO_2 \rightarrow ROOH + O_2$$
 (R21)

and by reactions in which both radicals and NO_x are lost:

$$OH + NO_2 + M \rightarrow HNO_3 + M \tag{R22}$$

$$RC(O)O_2 + NO_2 \leftrightarrow RC(O)O_2NO_2$$
 (R23)

$$RO_2 + NO \rightarrow RONO_2$$
 (R14b)

Reactions (R18) through (R21) are predominant when NO_x concentrations are low. Reactions (R22), (R23) and (R14b) become important when NO_x are high. The products of H_2O_2 , ROOH, HNO_3 and $RONO_2$ should be viewed as reservoirs, rather than terminal products, since they can lead to radical (or NO_x) regeneration, even with a small fraction, if they are not removed from the atmosphere by rainout or surface deposition. For example,

$$H_2O_2 + hV \rightarrow 2OH \tag{R24}$$

14 of 69th

$$ROOH + hv \rightarrow Carb + OH + HO_2$$
 (R25)

$$HNO_3 + hv \rightarrow OH + NO_2$$
 (R26)

Nitric acid (HNO₃), formed in (R22) and then most likely removed by heterogeneous process, is an effective sink for NO_x, at least in the planetary boundary. Peroxyacetyl nitrate (PAN) and its homologues formed via (R23) are thermally unstable and thus provide only the temporary reservoirs for NO₂. Most important, the lifetime of PAN becomes long enough at the colder temperatures of the middle and upper troposphere that it can be transported over long distances and serve as a carrier of NO_x into remote regions. Alkyl nitrates (RONO₂), which are formed in the alternative reaction path of RO₂ with NO (R14b) with small fraction (0.-0.15), could also provide a source of NO_x to more remote regions via photolysis or through reaction with OH following transport.

In addition to the reaction with OH (R22), heterogeneous losses of N_2O_5 also provide a sink for NO_x because of the thermal equilibrium established between NO_3 , NO_2 and N_2O_5 (R28) and, at the same time, results in the loss of ozone via (R27).

$$NO_2 + O_3 \rightarrow NO_3 + O_2 \tag{R27}$$

$$NO_2 + NO_3 \rightarrow N_2O_5 \tag{R28}$$

$$N_2O_5 + H_2O_{la} \leftrightarrow 2H^+ + 2NO_3^-$$
 (R29)

Above all, the photodissociation of O₃ and NO₂ are the driving forces for the chemical reactions on tropospheric ozone. The photodissociation rate coefficients of these reactions, i.e., J O₃(¹D) and J NO₂, are the most critical parameters in tropospheric chemistry [Thompson & Stewart, 1991]. To the first approximation, the ozone production increases with an enhancement of J_NO₂, since the increased J_NO₂ leads to the increase in the ratio of NO/NO₂, which favors the ozone production through reactions (R11) and (R14a) and reduces the chance of NO_x being removed via reaction (R22); and ozone destruction increases with an enhancement of J O₃(¹D), mainly due to the effective photolysis of ozone itself, i.e., reaction (R1) followed by (R2). However, the response in the net production of ozone to changes in J_values is more complicated. For example, while the effective photolysis of ozone, reaction (R1) followed by (R2), is the dominant contribution to the loss of ozone in the lower-to-middle troposphere, it also initiate the oxidation of CO and hydrocarbons (R9 and R12) and leads to the formation of peroxyl radicals, HO₂ and RO₂ (R10, R13 and R15), which may results in the ozone formation with the NO_x available (R11, R14a, R6 and R7). In addition to O₃ and NO₂, the photolysis of other species may also play an role in the chemical ozone budget. For example, the increase in J_values of aldehydes will results in more HO₂ and RO₂

TNO-MEP – R 96/406 15 of 69th

without consumption of OH or other radicals (R17a) and, thereby, increase production of ozone through reactions (R11) and (R14a).

TNO-MEP - R 96/406 17 of 69th

3. Model Description

3.1 Radiation Model

The radiation model adopted in this study is a delta-Eddington radiative transfer model, and originated from Madronich [1987] for calculations of the actinic flux and photodissociation rate coefficients in the troposphere [Ma, 1996].

The vertical profiles of temperature and air density are adopted from McClatchey et al. [1972] for mid-latitude summer conditions. The vertical profiles of ozone are adopted from a 1-D steady-state stratospheric model [Ma, 1992 & 1995], corresponding to projected reductions in stratospheric ozone for the perturbations in the study. When the effect of ozone as pollutant in the troposphere is considered, the tropospheric ozone profile used in the radiation model is from calculation by extended PHATIMA 1-D model for the industrialized rural areas [Ma, 1996]. The aerosol vertical profiles are originally from McClatchey et al. [1972], and are scaled to ones with optical parameters applied to the clean atmosphere and the polluted atmosphere, respectively [Ma, 1996]. The tropospheric sulfur dioxide (SO₂) profile for the polluted atmosphere is from the calculation by the PHATIMA 1-D model as well [Ma, 1996]. The homogeneous flat-layered clouds are assumed with the vertical location and optical properties according to Matthijsen [1995].

A summary of optical parameters for the reference and perturbed atmospheres is listed in Table 1. The calculations are carried out at Northern middle latitude (45°N) for averaged summer conditions (July 21) with a solar zenith angle of 24.5° at noon. The surface albedo is assumed to be 0.05, and to be wavelength-independent.

Table 1 The parameters adopted in the radiation model for the reference atmosphere and the perturbated atmospheres.

Reference	Atmosphere	
REF0		
Ozone(O ₃):	stratospheric column,	295.8 D.U.
	tropospheric column,	32.1 D.U.
Sulfur dioxide (SO ₂):	total column,	0.0 D.U.
Aerosols:	optical thickness,	τ=0.21
	single-scatter albedo,	ω =0.99
	asymmetry parameter,	g=0.70
Clouds:	optical thickness,	τ=0.00
	single-scatter albedo,	ω =0.9999
	asymmetry parameter,	g=0.875
Cloudy Atmosphere: Same a	s REF0, except for Clouds	
CDM1 (thin and middle);	optical thickness(4-4.5km),	τ= 2.
CDM2 (thick and middle);	optical thickness(4-4.5km),	τ =10.
CDL1 (thin and low);	optical thickness(1-1.5km),	τ =10.
CDL2 (thick and low);	optical thickness(1-1.5km),	τ=50.
Stratospheric Ozone Depletic	on: Same as REF0, except for Ozone	
OZD1 (by 5%);	stratospheric column,	288.4 D.U.
OZD2 (by 10%);	stratospheric column,	281.0 D.U.
OZD3 (by 15%);	stratospheric column,	273.6 D.U.
OZD4 (by 20%);	stratospheric column,	266.2 D.U.
D2L1; The combination of O	ZD2 and CDL1	
Tropospheric Pollution: Same	e as REF0, except for	
PLO1; Ozone(O ₃):	tropospheric column,	50.1 D.U.
PLS1; Sulfur dioxide (SO ₂):		2.5 D.U.
PLA1; Aerosols:	optical thickness,	$\tau = 0.54$
	single-scatter albedo,	ω=0.87
PASO; The combination of I	_	

3.2 Extended PHATIMA

The PHATIMA 1-D model is an adapted version of a 1-D model developed at NOAA (Trainer et al., 1987; McKeen et al., 1989; Trainer et al. 1991). The adaption has been made at TNO for photochemistry with vertical transport in the troposphere over the continent and the ocean in the 30°-60°N zonal band [Meijer et al., 1994; Matthijsen, 1995]. The PHATIMA 1-D model has been approved to be a very effective tool for the study of chemical processes in the whole troposphere over the clean region or merely the boundary layer of the polluted region. However, the model simulation by PHATIMA is not so satisfied for the upper troposphere over the polluted region like eastern United States and western Europe, since the calculted concentrations of, e.g., NO_x and O₃, are much higher than the realistic ones (see Figure 1).

TNO-MEP - R 96/406 19 of 69th

An extended version of the PHATIMA 1-D model has been developed for the study of chemical processes in the troposphere over different chemical coherent regions, the polluted region in particular [Ma, 1996]. This extended PHATIMA does simulation for the ocean, the clean continent and the polluted continent in the 30°-60°N zonal band simultaneously. In the model, the horizontal exchanges of trace gases in the free troposphere among the three regions occur periodically after certain days of simulation , while the planetary boundary layers of these regions are treated in isolation with each other. In addition, the $\rm NO_x$ sources from lightnings and subsonic aircrafts, which were not considered before, are also incorperated into the model.

Table 2 The surface emission rates for different regions in the extended PHATIMA (in $cm^{-2} \cdot s^{-1}$).

Species	Ocean	Clean Continent	Polluted Continent
NO _x	1.3×10 ⁸	1.0×10 ¹⁰	2.5×10 ¹¹
CO	1.0×10 ¹¹	2.0×10 ¹¹	1.8×10 ¹²
C ₂ H ₆	1.0×10 ⁸	1.2×10 ¹⁰	6.0×10 ¹⁰
C ₃ H ₈	5.0×10 ⁸	1.5×10 ¹⁰	7.5×10^{10}
C ₄ H ₁₀	1.0×10 ⁹	2.0×10 ¹⁰	1.0×10 ¹¹
C ₂ H ₄	4.5×10 ⁹	1.8×10 ¹⁰	9.0×10^{10}
C ₃ H ₆	6.0×10 ⁹	1.5×10 ¹⁰	7.5×10 ¹⁰
Toluene	_	2.0×10 ⁹	1.0×10 ¹¹
Isoprene	_	5.4×10 ¹⁰	5.4×10 ¹⁰
SO ₂	-	2.9×10 ¹⁰	1.4×10 ¹¹

The concentrations of methane (CH₄) and molecular hydrogen (H₂) are kept constant for all regions in the model, with 1.7 ppmv for CH₄ and 500 ppbv for H₂, respectively.

Table 3 The daily averaged surface concentrations of some species at the last day of initial simulation (in ppbv).

Species	Ocean	Clean Continent	Polluted Continent
NO _x	.023	.307	3.86
CO	95.7	113.	197.
C ₂ H ₆	1.17	2.35	4.50
C ₃ H ₈	.175	1.09	3.08
C ₄ H ₁₀	.092	.868	2.82
C ₂ H ₄	.131	.385	1.43
C ₃ H ₆	.081	.183	.639
Toluene	_	.051	.184
Isoprene	_	.285	.231
H ₂ O ₂	.863	1.39	2.15
CH ₂ O	.292	.862	1.96
HNO ₃	.080	.389	3.22
O ₃	26.6	30.0	50.9

20 of 69th

In the model, a 20 days' initial running has been conducted for the ocean, clean continent and polluted continent simultaneously so that a periodic diurnal variation of chemical species concentrations are approached for these regions [Ma, 1996]. The surface emission flux of species for the ocean, clean continent, and polluted continent in the extended version of PHATIMA is given in Table 2. The daily averaged surface concentrations of some species at the last day of initial simulation is shown in Table 3. The vertical distributions of nitrogen oxides, NO_x, and ozone, O₃ over the regions of the ocean, clean continent and polluted continent at that day are shown in Figure 1. In addition, water vapor is also very important for the chemical budget of ozone in the troposphere. The water vapor profiles at noon under the clear-sky and a cloudy (low clouds: st/sc) conditions used in the model are shown in Figure 2 for the ocean and the continent, respectively. For the purpose of this study, 5 more days simulations are carried out after the initial running with the specific radiation field due to varied clouds, ozone column and tropospheric pollutants as shown in Table 1.

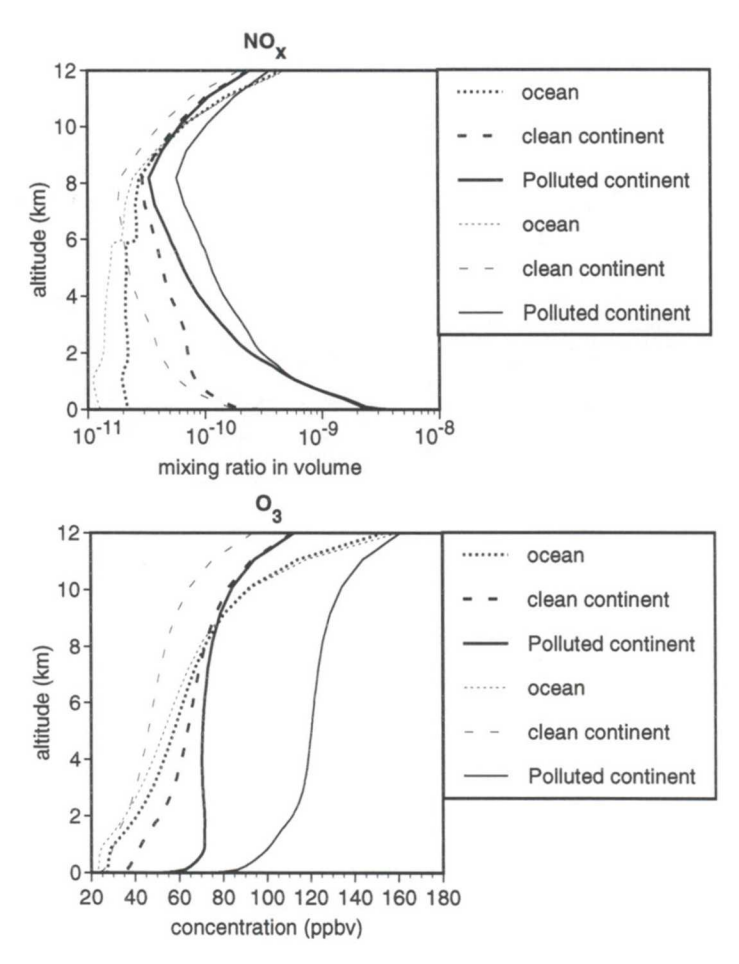


Figure 1 The vertical distributions of the daily averaged concentrations of nitrogen oxides (NO_x) and ozone (O_3) at the last day of the initial running (heavy lines). For comparison, the results from the adapted PHATIMA are also shown (weak lines).

TNO-MEP - R 96/406 21 of 69th

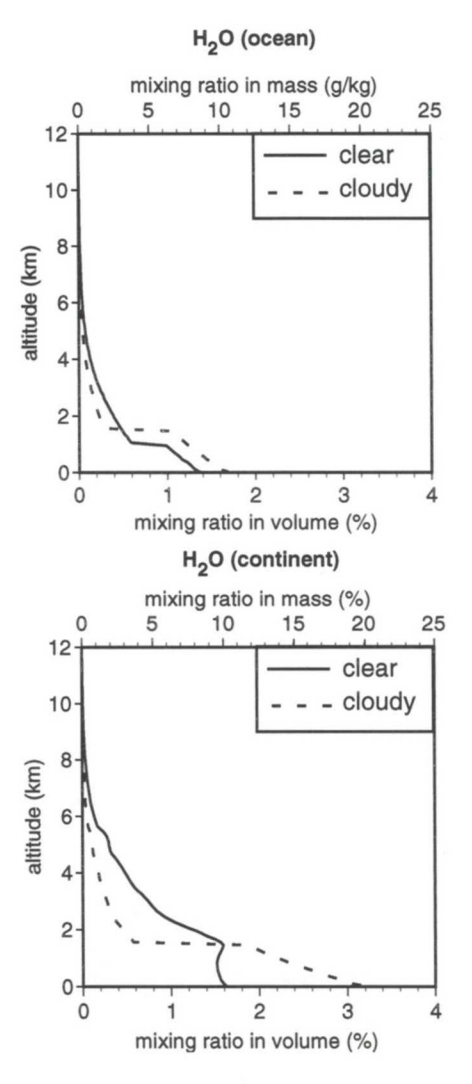


Figure 2 The water vapor profiles at noon under the clear-sky and a cloudy (low clouds: st/sc) conditions for the ocean and the continent.

TNO-MEP - R 96/406 23 of 69th

4. Results and Discussion

In this section, the effects of radiation changes on photodissociation rate coefficients of the species, the net ozone production, and the relevant chemical reactions, are studied for 5 days perturbations due to clouds, stratospheric ozone depletion, and tropospheric pollution, respectively, with reference to a clear sky condition (Table 1.).

4.1 J values

4.1.1 Effect of clouds

The effect of clouds on actinic flux and hence photo-dissociation rate coefficients (J_values) in the troposphere has been studied previously [e.g., Madronich, 1987; Van Weele and Duynkerke, 1993; Matthijsen, 1995]. Figure 3 shows the calculated changes in J_NO₂ and J_O₃(¹D) at noon (solar zenith angle = 24.5°) with clouds relative to a clear sky condition. Due to the spectral effects by ozone absorption and Rayleigh scattering, the effect of clouds as well as column ozone on J values is wavelength-dependent and different for different species [Thompson, 1984; Ma, 1995; Matthijsen, 1995]. In the figure, only changes in J_values of NO₂ and O₃ are given. This is because, first, the NO₂ and O₃ are the most important species for the photolysis process in the troposphere [Thompson and Stewart, 1991]. Second, the changes in J values of other species, except for J_NO₃, falls in the range of variations between J_NO₂ and J_O₃(¹D).

Matthijsen [1995] has shown the importance of altered water vapor concentrations during cloudy conditions for the chemical ozone budget. Since reaction (R2) is the effective path for the photolysis of ozone to produce OH, the effective photodissociation rate coefficient of ozone, $J_0_3(^1D)_{eff}$, is expressed in terms of $J_0_3(^1D)$ and the fraction of exited oxygen atoms that react with water vapor, $f(q_v)$ [WMO, 1995; Van Weele, 1996],

$$J_{Q_3}(^1D)_{eff} = J_{Q_3}(^1D) \cdot f(q_v)$$
 (F1)

where

$$f(q_{\nu}) = k_2[H_2O]/(k_2[H_2O] + k_3[M])$$
(F2)

With reference to Van Weele [1996], given the reaction rates of (R2) and (R3) and the specific humidity q_v (g/kg), $f(q_v)$ can be written as the following

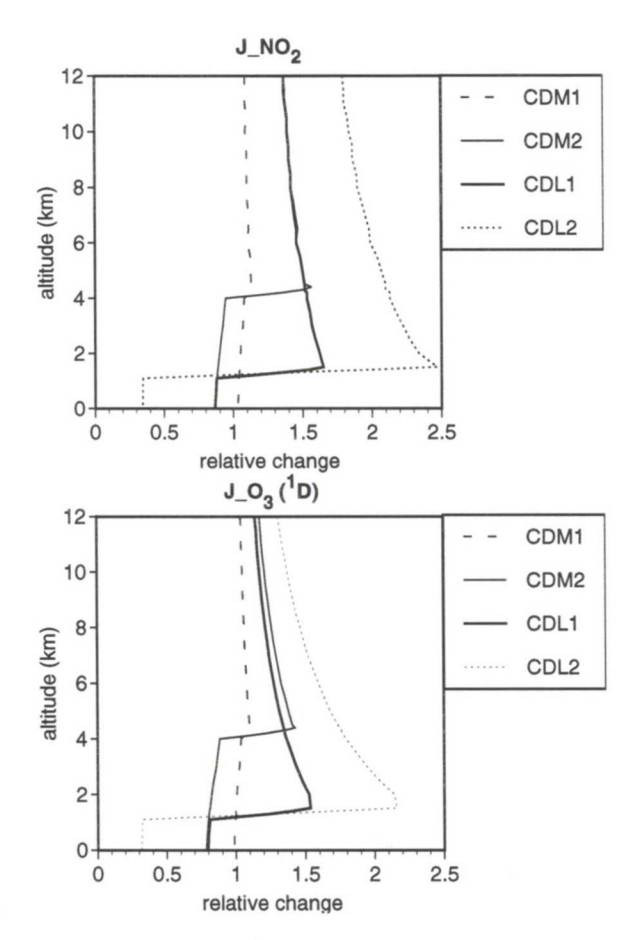


Figure 3 The changes in J_NO_2 and $J_O_3(^{1}D)$ with clouds relative to the clear-sky condition (REF0).

$$f(q_{\nu}) = q_{\nu}/(q_{\nu} + 81.1)$$
 (F3)

Therefore, the effect of variation in water vapor during cloudy conditions is included in $J_O_3(^1D)_{\text{eff}}$. According to Mattijsen [1995], for the low clouds (st/sc), the water vapor below and in the cloud is assumed to be saturated (relative humidity: rh = 100%), whereas above the cloud the air is assumed to be dry (rh = 20%) (see Figure 2). For the middle clouds, the water vapor below and above the cloud is assumed to be the same as in the clear sky, whereas in the cloud the air is assumed to be saturated. The changes in $J_O_3(^1D)_{\text{eff}}$ at noon with clouds are shown Figure 4 for the ocean and continent, respectively.

One can see that the influence of variation in $f(q_v)$ on $J_O_3(^1D)_{eff}$ is so significant that it dominates over the variation in $J_O_3(^1D)$ itself for certain situation. Under the thin low cloud (CDL1), for example, there is an increase in $J_O_3(^1D)$ above the

TNO-MEP - R 96/406 25 of 69th

cloud, whereas $J_O_3(^1D)_{,eff}$ is decreased. The decrease in $J_O_3(^1D)_{,eff}$ below the clouds is smaller than that of $J_O_3(^1D)$, and even there is an increase in $J_O_3(^1D)_{,eff}$ below the clouds over the continent. Since the water vapor above and below the middle cloud is assumed to be the same as in the clear sky, the effect of thinnest middle clouds (CDM1) on J values is negligible except that $J_O_3(^1D)_{,eff}$ in the cloud is considered.

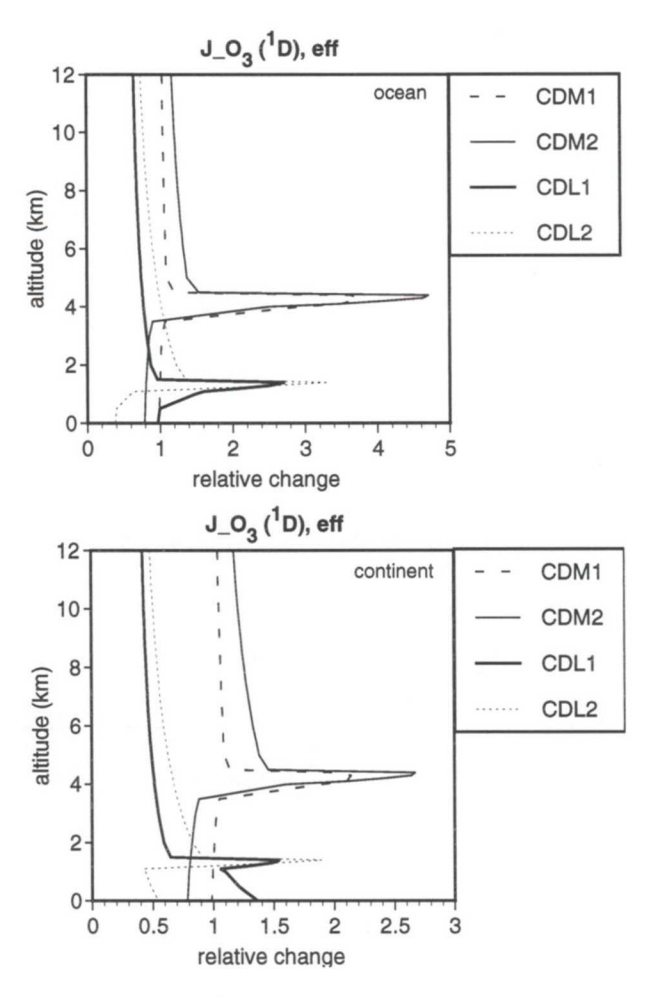


Figure 4 The changes in $J_0^{(d)}D$), eff with clouds over the ocean and the continent relative to the clear-sky condition (REF0).

4.1.2 Effect of stratospheric ozone depletion

The contribution of the spectral J_value to the total J_value at specific wavelength is species-dependent. Therefore, the sensitivity of the responses of J_values to stratospheric ozone depletion, which enhances the actinic flux only in the UV-B region through the troposphere, varies significantly for different species [Fuglestvedt, 1994; Ma, 1995]. To quantify the sensitivity of the responses, the J_value Amplification Factor (JAF) for stratospheric ozone depletion can be de-

fined. Ma [1995] calculated the sensitivity factor in terms of a relative increase in the photodissociation rate coefficient of a specific species (J_i) for a relative decrease in the stratospheric ozone column (O_3) :

$$JAF_i = -(\Delta J_i/J_i)/(\Delta O_3/O_3) \tag{F4}$$

This expression is a linear relationship. However, when stratospheric ozone depletion varies greatly, there is a large deviation in the calculated JAF, for $J_0_3(^1D)$ in particular, with this definition (Figure 5). If the definition in (F4) is applied to the large depletion in ozone, the magnitude of the deduced increase in J_v alues is underestimated. To avoid this problem, initiated by Madronich [1993], a reformed expression in terms of a power law is adopted best for the definition of JAF:

$$JAF_{i} = ln(J_{i}^{*}/J_{i})/ln(O_{3}/O_{3}^{*})$$
 (F5)

where J_i^* and J_i are the values of photodissociation rate coefficient of a specific species corresponding to amounts of ozone column O_3^* and O_3 above, respectively. Figure 5 shows that the JAF for $J_iO_3(^1D)$ calculated with the definition in (F5) agrees very well for different stratospheric ozone depletions. As shown in Figure 6, the effect of stratospheric ozone depletion on the J_i values is almost homogeneous through the troposphere.

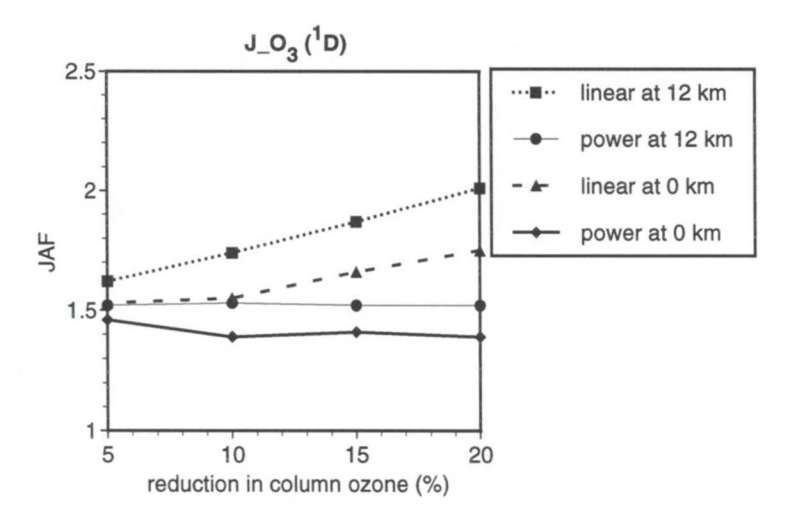


Figure 5 The dependence of the J_{value} Amplification Factor (JAF) for O_3 on the change in column ozone due to stratospheric ozone depletion.

The calculated average of JAF of selected species in terms of power law (F5) for stratospheric ozone depletion are given in Table 4. The deviation of JAF for O₃ between the tropopause and the surface is about 0.07, and even smaller for other species. Like clouds, the effect of stratospheric ozone depletion on J_values is also different for different species due to the spectral characteristics of molecular ab-

TNO-MEP - R 96/406 27 of 69th

sorption. As shown in the table, the J_0^1D is only one with JAF bigger than unit while the responses of some J values, such as J NO_2 , is negligible.

Table 4 The average of J_value Amplification Factor (JAF) through the troposphere calculated with (F5).

J_Species	JAF
J_O ₃ (¹ D)	1.45
J_HNO₃	0.89
J_HNO₄	0.59
J_CH ₃ CHO	0.73
J_CH ₃ COCH ₃	0.60
$J_N_2O_5$	0.30
$J_H_2O_2$	0.31
J _A _HCHO	0.38
J _B _HCHO	0.12
J_CH₃OOH	0.31
J_NO ₂	0.02
J_NO ₃	0.03
J_HNO ₂	0.01

The values in Table 4 are derived for the clear sky condition. Some runs under the cloudy conditions assumed in this study are carried out, and the result is the same as for the clear sky condition with respect to the deviation for the values in the table. This implies that the paramerization of effects of clouds and ozone column can be carried out independently.

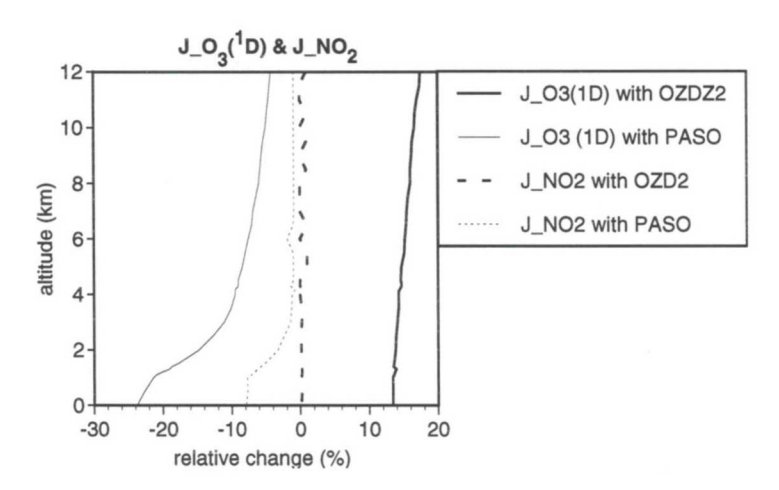


Figure 6 The changes in J_NO_2 and J_NO_3 and J_NO_3 due to stratospheric ozone depletion (OZD2) and due to tropospheric pollution (PASO) relative to the clean atmosphere (REF0), respectively.

28 of 69th

4.1.3 Effect of tropospheric pollution

To study the possible effect of tropospheric pollutants on the chemical budget of ozone in the troposphere through radiation changes, the photodissociation rate coefficients are re-calculated by including more ozone (O_3) , sulfur dioxide (SO_2) , and aerosols (PLO1, PLS1, PLA1, and PASO in Table 1) in the troposphere, respectively. The calculated variations in $J_0_3(^1D)$ and J_0_2 due to the combined effect (PASO) of tropospheric pollutants, i.e., O_3 , SO_2 and aerosol, relative to the reference case (REF0) are shown in Figure 6 with comparison to the effect of statospheric ozone depletion. One can see that the effect of tropospheric pollution occurs mostly in the lower troposphere, which can offset the increase in $J_0(^1D)$ due to stratospheric ozone depletion in the boundary layer.

Individual calculations with PLO1, PLS1, and PLA1 show that the effects of O_3 and aerosols on $J_O_3(^1D)$ are comparable, while the effect of SO_2 is smaller due to the less amount of SO_2 in the troposphere. The effects of the aerosols on J_NO_2 and $J_O_3(^1D)$ are different with much more decrease in $J_O_3(^1D)$ than in J_NO_2 . The decrease in J_NO_2 with PASO in Figure 6 is attributed to the effect of aerosols, since the effect of O_3 and O_2 on O_3 is neligible.

4.2 Net Ozone Production

Since the concentrations of ozone precursors, such as NO_x, CO and NMHC_s, and ozone itself as well as the climatology, e.g., water vapor and clouds, vary significantly from region to region, the chemical budget of ozone are quite different in both spatial and temporal sense. Figure 7 shows the net chemical production of ozone, i.e., P-L, above the ocean, clean continent and polluted continent for a clear sky condition (REF0, in Table 1.). In the upper troposphere, the chemical ozone production is larger than the chemical ozone destruction i.e., P-L>0, for all regions. In the middle troposphere, the chemical production and destruction tend to be in balance, i.e., P-L≈0. The altitude range at which this balance occurs depends on the in-situ amount of precursors and ambient climateoroloy and thus varies with different regions and radiation fields. In the lower troposphere, the chemical budget varies greatly from region to region. There are always a net destruction of ozone, i.e., P-L<0, over the ocean and a net production of ozone, i.e., P-L>0, over the polluted continent in the lower troposphere. Over the clean continent, ozone is net produced, i.e., P-L>0, in the lower boundary layer, and net destructed, i.e., P-L<0, in the upper boundary layer and lower free troposphere.

TNO-MEP - R 96/406 29 of 69th

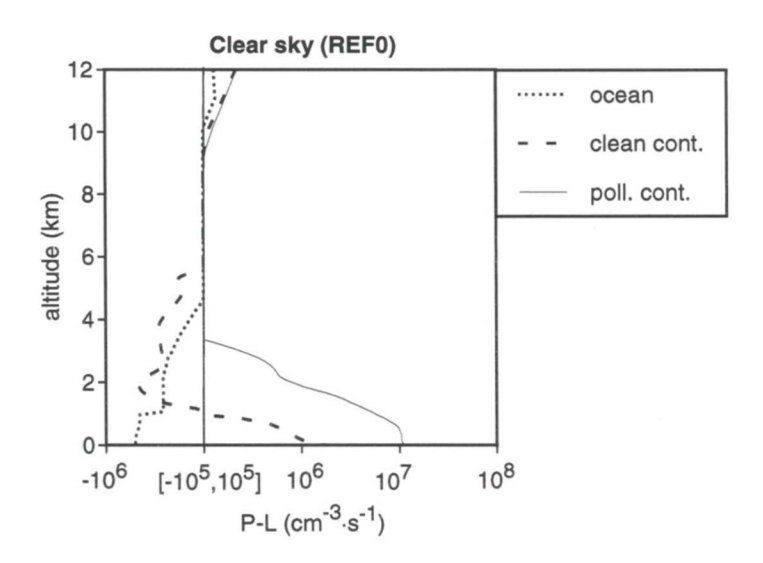


Figure 7 The local net production of ozone, P-L, in the troposphere over the ocean, the clean continent and the polluted continent under the clear-sky condition (REF0).

4.2.1 Effect of clouds

In Figure 8, the changes in the local net chemical production of ozone, i.e., $\Delta(P-L)$, due to the perturbations of clouds are shown for the oceanic, clean continental and polluted continental regions, respectively. Since J_NO_2 increases more efficiently than $J_O_3(^1D)$ above the clouds and, even more, $J_O_3(^1D)$,_{eff} may decrease due to the less water vapor above the low clouds (CDL1 and CDL2) as shown in Figure 3 and Figure 4, the net ozone production increase above the clouds for all regions. As the water vapor in the clouds is saturated, $J_O_3(^1D)$,_{eff} increases profoundly with respect to the clear sky condition. Therefore, the net production of ozone decreases in the clouds for all cases of this study.

Below the clouds, the change in the net ozone production also depends on the ambient conditions. Over the ocean (Figure 8a), there is a net destruction of ozone in the lower troposphere, i.e., P-L<<0, and the change in the chemical ozone destruction due to $J_O_3(^1D)_{\text{eff}}$ predominates the change in the chemical ozone production due to J_NO_2 . Therefore, the net production of ozone is increased due to the decrease in $J_O_3(^1D)_{\text{eff}}$. For example, the $J_O_3(^1D)_{\text{eff}}$ decrease more with the thick low clouds (CDL2: τ =50 at 1-1.5 km) than with the thin low clouds (CDL1: τ =10 at 1-1.5 km), and hence the net production of ozone for CDL2 increases more than that for CDL1 below the clouds.

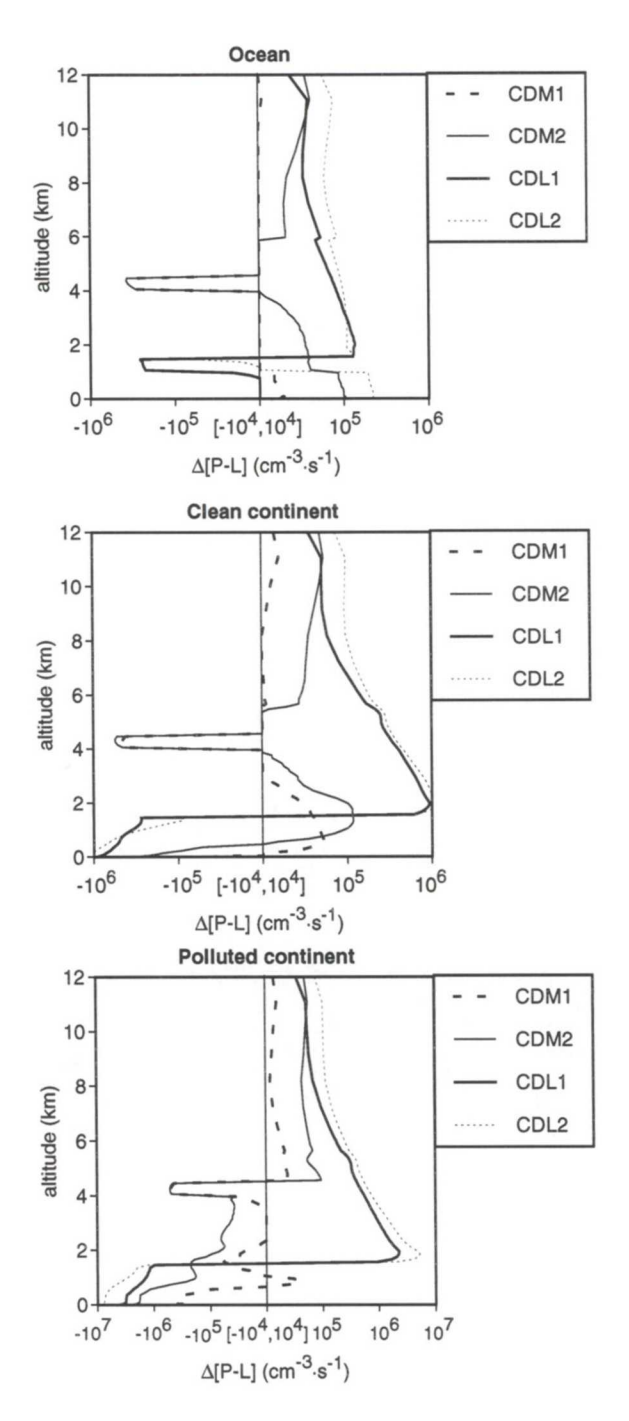


Figure 8 The difference in the local net production of ozone, $\Delta(P-L)$, due to clouds with respect to the clear-sky condition (REF0).

Over the continent (Figure 8b,c), the situation below the clouds is more complicated due to varied chemical coherent region and different clouds. In the continental boundary layer, particularly near the surface, the chemical ozone production is larger than the chemical ozone destruction, i.e., P-L>0, and the change in J_NO_2 predominates over the change in $J_O_3(^1D)_{\text{eff}}$ with respect to the trend of the net

TNO-MEP - R 96/406 31 of 69th

production of ozone. Therefore, in the continental boundary layer, the net ozone production decreases below the clouds mainly due to the decrease in J_NO_2 . Below the middle clouds (CDM1 and CDM2), the lower free troposphere and upper boundary layer are also included, where the ozone is net destructed over the clean continent but net produced over the polluted continent. Below the thick middle clouds (CDM2: τ =10 at 4-4.5 km), for example, since no change in water vapor is assumed below the middle clouds, $J_NO_3(^1D)_{\text{eff}}$ is the same as $J_NO_3(^1D)_{\text{eff}}$ and both J_NO_2 and $J_NO_3(^1D)_{\text{eff}}$ decrease relative to the clear sky condition. However, the net production of ozone below the thick middle clouds is increased over the clean continent due to a decrease in $J_NO_3(^1D)_{\text{eff}}$, and decreased over the polluted continent due to a decrease in J_NO_2 .

The variations in column integrated rate of the net ozone production with clouds are shown in Figure 9 for the boundary layer, free troposphere and whole troposphere of all three regions, respectively.

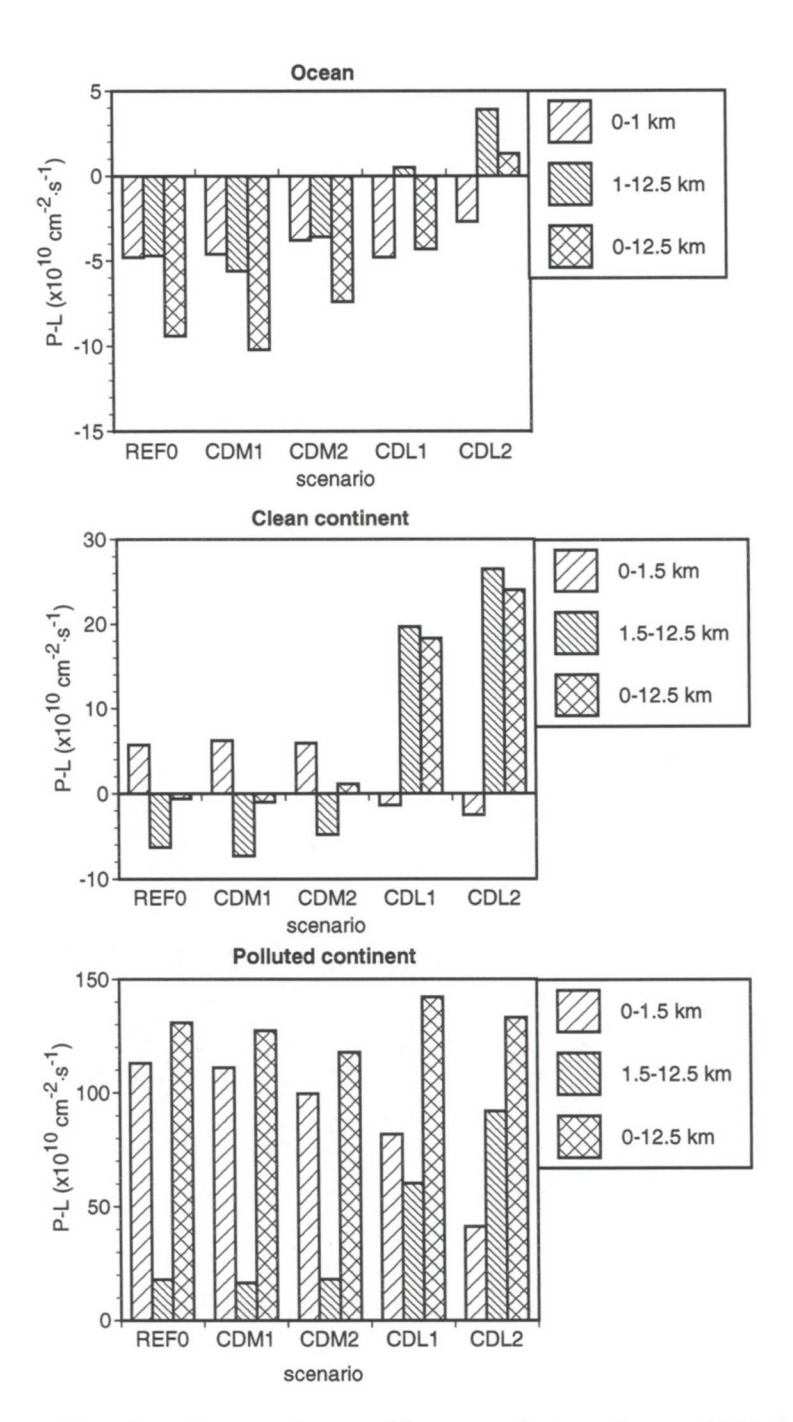


Figure 9 The column integrated rates of the net production of ozone, (P-L), for the boundary layer, the free troposphere and the whole troposphere with different clouds.

TNO-MEP - R 96/406 33 of 69th

Ocean

One can see from Figure 9a that ozone is net destructed under the clear-sky condition over the ocean, with nearly the same contribution from the boundary layer and from the free troposphere. The net destruction of ozone changes slightly with the thin middle cloud (CDM1: τ =2 at 4-4.5 km) and decreases with the thick middle cloud (CDM2: τ =10 at 4-4.5 km) in both the boundary layer and the free troposphere. There is almost no change with the thin low cloud (CDL1: τ =10 at 1-1.5 km) but a decrease with the thick low cloud (CDL2: τ =50 at 1-1.5 km) for the net destruction of ozone in the boundary layer. The net destruction of ozone in the free troposphere decreases significantly and even turns to be net produced with the low clouds (CDL1 and CDL2). Therefore, for the whole troposphere over the ocean, the net destruction of ozone tends to decrease with the clouds, especially with the low clouds (CDL1 and CDL2). There is an exception for the thin middle cloud (CDM1), the perturbation of which is relatively small.

Clean continent

As shown in Figure 9b, under the clear-sky condition over the clean continent, ozone is net produced in the boundary layer and net destructed in the free troposphere which offset each other. As a result, there is a very small net destruction of ozone in the whole troposphere. Both the net production of ozone in the boundary layer and the net destruction of ozone in the free troposphere changes slightly with the middle clouds (CDM1 and CDM2: at 4-4.5 km). While the net production of ozone in the boundary layer turns to be net destructed with the low clouds (CDL1 and CDL2: at 1-1.5 km), the net destruction of ozone in the free troposphere switches to be net produced even to a larger extent. Therefore, for the whole troposphere over the clean continent, the net production of ozone changes slightly with the middle clouds (CDM1 and CDM2), and increases significantly with the low clouds (CDL1 and CDL2) relative to the clear-sky condition.

Polluted continent

As shown in Figure 9c, ozone is always net produced both in the boundary layer and in the free troposphere over the polluted continent. There is a decrease in the net production of ozone in the boundary layer with the thick middle cloud (CDM2: τ =10 at 4-4.5 km). With the low clouds (CDL1 and CDL2: at 1-1.5 km), the net production of ozone decreases in the boundary layer and increases in the free troposphere. For the whole troposphere over the polluted continent, the net production of ozone tends to decrease with both the middle clouds (CDM1 and CDM2) and to increase with the low clouds (CDL1 and CDL2) relative to the clear-sky condition.

Summary

In priciple, the net destruction of ozone can also be represented by the net productiuon of ozone with a negative sign. The effect of the thin middle cloud (CDM1: τ =2 at 4-4.5 km) on the net production of ozone is small for all cases. With the thick middle cloud (CDM2: τ =10 at 4-4.5 km), the net production of ozone increases sligtly in both the boundary layer and the free troposphere of the ocean and

in the free troposphere of the clean continent, but decreases in the boundary layer of the polluted continent. With the low clouds (CDL1 and CDL2: at 1-1.5 km), the net production of increases in the free troposphere of all regions, but decreases in the boundary layer of the clean and polluted continents.

4.2.2 Effect of stratospheric ozone depletion

The changes in the local net chemical production of ozone, i.e., $\Delta(P-L)$, due to stratospheric ozone depletion are shown in Figure 10 for the oceanic, clean continental, and polluted continental regions, respectively. The sensitivity of the response in J_values to the perturbation due to stratospheric ozone depletion is quite species-dependent, with the highest for $J_0^{-1}(D)$ and the neligible for $J_0^{-1}(D)$ and the neligible for $J_0^{-1}(D)$ and the neligible for J_NO2 (Table 4). Therefore, the net production of ozone tends to decrease with stratospheric ozone depletion even on a continental scale. This is because the increase in the photolysis of ozone itself increases which, to the first approximation, favors the ozone destruction as the amount of NO_x is limited in most regions. Since the effective photolysis of ozone occurs only when the water vapor is available, instead of $J_0^{-1}(D)$, $J_0^{-1}(D)$, $J_0^{-1}(D)$, seff should be considered for the study on tropospheric chemistry.

The trend of the net production of ozone with stratospheric ozone depletion is the same for all regions in the free troposphere (Figure 10a,b,c). In the upper free troposphere, the response is negligible since the concentrations of water vapor there are very low and the $J_0(1^{-1}D)_{eff}$ as well as its variation plays a small role in the chemical budget of ozone. In the lower free troposphere, the net destruction of ozone for the ocean and the clean continent increases, and the net production of ozone for the polluted continent decreases. This is because the concentrations of water vapor there are high and the effective of the photolysis of ozone itslf becomes dominant in the chemical budget of ozone over the ocean, or comparable to the chemical ozone production over the continent.

In the boundary layer of the ocean (Figure 10a), the net destruction of ozone increases more than in the lower free troposphere, since the concentration of water vapor is higher and thus the effective photololysis of ozone, which is dominant in the chemical budget of ozone over the ocean, increases significantly there. Over the boundary layer of the continent (Figure 10b,c), the situation is complicated since the role of NO_x is also important and even turns to be dominant for the chemical budget of ozone there. Over the clean continent (Figure 10b), the net destruction of ozone in the upper boundary layer increases, and the net production of ozone in the lower boundary layer decreases. And this decrease becomes less and less down to the surface, since the role of NO_x becomes important for the chemical budget of ozone near the surface of the clean continent. Over the polluted continent (Figure 10c), the net production of ozone still decreases in the upper boundary layer, but turns to increase in the lower boundary layer. And this increase is attributed to the

TNO-MEP - R 96/406 35 of 69th

fact that the increase in the ozone production, via the enhancement of peroxy radials, predominates over the increase in the ozone destruction, via the effective photololysis of ozone itself, as NO_x instead of water vapor is dominant for the chemical budget of ozone in the lower boundary layer of the polluted continent.

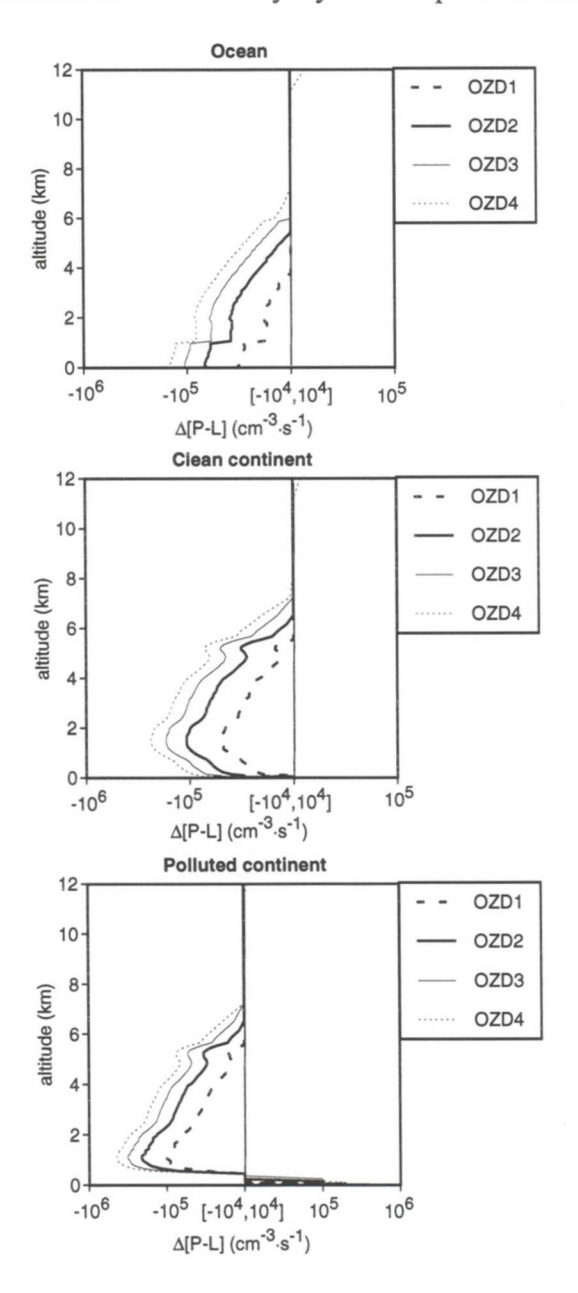


Figure 10 The difference in the local net production of ozone, $\Delta(P-L)$, due to stratospheric ozone depletion with respect to the clear-sky condition (REF0).

The variations in column integrated rate of the net ozone production with projected reductions in stratospheric ozone are shown in Figure 11 for the boundary layer, free troposphere and whole troposphere of all three regions, respectively. One can see that the net production of ozone decreases in both the boundary layer and the

free troposphere over all regions. In a relative sense, the decrease is significant over the ocean and the clean continent (Figure 11a,b), and very small over the polluted continent, the polluted boundary layer in particular (Figure 11c). The changes in the net production of ozone are nearly proportional to the reductions in stratospheric ozone for a specific region.

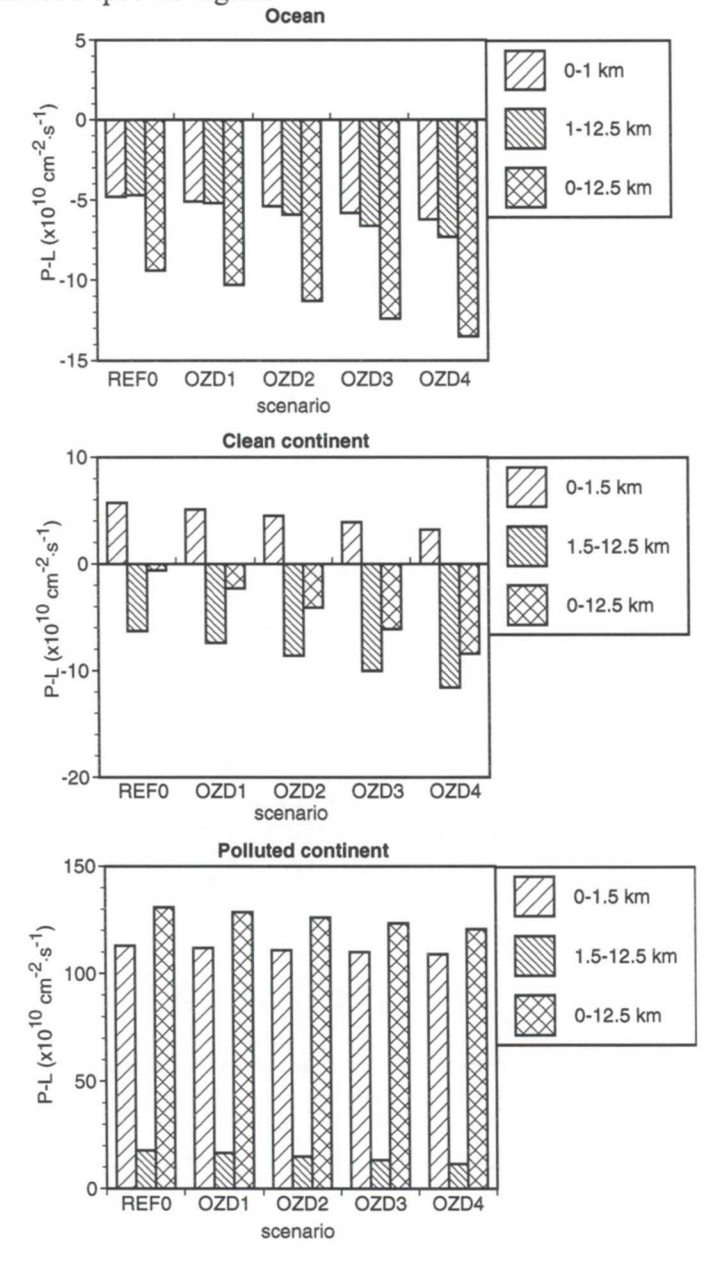


Figure 11 The column integrated rates of the net production of ozone, (P-L), for the boundary layer, the free troposphere and the whole troposphere with different stratospherioc ozone depletions.

TNO-MEP - R 96/406 37 of 69th

Polluted boundary layer

The results above are consistent with those expected by Liu and Trainer [1988] and Thompson et al. [1989] for the ocean and the clean continent. For the boundary layer of the polluted continent, however, the net production of ozone still decreases slightly according to the calculation by PHATIMA, which seems contradictory to the conclusion from former studies.

To distinguish the results between different calculations, one should note that the models, methods and ambient conditions used are completely different. The model that Liu and Trainer [1988] used is a box model, and the concentrations of ozone precursors, namely NO_x, NMHC_s, CH₄, and CO, are fixed in their simulations. As they mentioned, the chemical production of ozone is over-estimated due to neglecting the feedback of OH enhancement and additional sinks of NO_x and NMHC_s. Therefore, the perturbation of O₃ at high NO_x levels should be scaled accordingly in their results. Thompson et al. [1989] did use an one-dimensional model, but only ethane (C₂H₆) with a fixed concentration is included as NMHC_s in their model. For the polluted continent of this study, at the last day of the initial simulations the NO_x concentration is about 3.9 ppbv at the surface and much lower in the upper boundary layer (e.g., 0.35 ppbv at 1.5 km), with an average of around 1.0 ppbv for the whole boundary layer (0-1.5 km). In the model of Thompson et al. [1989], the NO_x concentration is lower at the surface (1.4 ppbv), but may be higher in the upper boundary layer and free troposphere, as NO_x can be accumulated at high altitude over the polluted region when the horizontal transport is neglected in their steady-stae 1-D model. Because of the non-linear relationship between the ozone production and the NO_x levels [Liu et al., 1987; Lin et al., 1988], the ozone production must have been over-estimated for the smaller gradient of the NO_x concentrations through the boundary layer. In addition, the water vapor profiles are also different between the models. The averaged relative humidity in the boundary layer is approximately 45% in Thompson et al.'s model and 70% in the Extended PHATIMA of this study. At the altitudes of about 1-1.5 km, the relative humidity can reach as much as 80% for the clear sky condition of this study. Since the basic structures are quite different between the models, the re-simulations with the Extended PHATIMA by using the same conditions as the former studies may be no possible. However, to argue that in addition to the local NO_x levels, the ambient concentrations of NMHC_s and water vapor also play an role in the response of tropospheric ozone to stratospheric ozone depletion, a few more situations for the polluted continents are assumed and examined.

As shown in Table 5, various cases of NO_x and $NMHC_s$ emissions are projected for the different polluted regions. The case EMS0 is the base one, which has been assumed to be typical for the polluted continents normally in this study. The case EMS1 is assumed just as same as Thompson et al.'s [1989] treatment of $NMHC_s$. The case EMS2 and EMS3 are projected to see the situations of the higher NO_x level with different $NMHC_s$ conditions. The simulations by the extended PHATIMA are still carried out for 20 days initial runs and then 5 days perturba-

tions. For the perturbation due to stratospheric ozone depletion, a 10% reduction in stratospheric ozone is considered for both the clear-sky condition (OZD2 relative to REF0) and a cloudy condition (D2L1 relative to CDL1). The calculated concentrations of NO_x and O₃ at selected altitudes under the clear sky condition (REF0) are given in Table 6 for each case. The surface NO_x concentrations are 15-17 ppbv for the higer NO_x cases (EMS2 and EMS3), which are possible in the downwind area of urban plume [Jacob et al., 1993a] and also comparable to the NO_x concentration in the rural area of The Netherlands [Van den Hout et al., 1990]. The surface ozone concentration is 53 ppbv for the lower NO_x and higher NMHC_s case, i.e., the base case (EMS0), and increases to 59 ppbv for the higer NO_x and higher NMHC_s case (EMS2), but decreases to 44 ppbv for the higer NO_x and lower NMHC_s case (EMS3). Therefore, the case EMS0 can represent for the NO_x limited region, and the case EMS3 for the NMHC_s limited region. The production of ozone in most industrialized rural areas are still limited by the availability of NO_x even in the boundary layer over the European and North American continents [WMO, 1995].

Table 5 The various cases of surface emissions of NO_x and $NMHC_s$ for the different polluted regions.

_	
EMS0:	Base case, with surface emissions given in Table 2 for the polluted continent;
EMS1:	Same as EMS0, but only C_2H_6 as NMHC _s , with an emission as same as in Table 2 for the clean continent;
EMS2:	Same as EMS0, but with a value of 1.0×10^{12} for the NO _x emission (four times more than EMS0);
EMS3:	Same as EMS2, but with a reduction of NMHC _s emissions (except for isoprene) by 60%.

Table 6 The concentrations of O_3 and NO_x at selected altitudes with various NO_x and $NMHC_s$ emissions for the different polluted regions. The results are for the clear-sky condition (REF0). (*)

case	EMS0	EMS1	EMS2	EMS3
O ₃ (at surface)	53	39	59	44
NO _x (at surface)	3.7	4.1	15.	17.
NO _x (at 1.5 km)	.36	.36	.95	1.3
NO _x (turning point)	1.4	0.7	1.7	1.3
(height in km)	(0.4)	(0.9)	(1.1)	(1.5)

^{*} In unit of ppbv, except for heights of turning point.

Figure 12a shows the change in the local net chemical production of ozone (up to the height of 1.5 km) with stratospheric ozone depletion for various cases of NO_x and $NMHC_s$ emissions under the clear-sky condition (see Table 5 and Table 6). In all cases, the net production of ozone is decreased in the upper boundary layer but increased in the lower boundary layer. Since the mixing ratio of water vapor, and thus $J_O_3(^1D)_{seff}$, over the continent is very large almost homogeneousely through the whole boundary layer (Figure 2b), the effective photolysis of ozone increases significantly with stratospheric ozone depletion in both the lower and the upper

TNO-MEP - R 96/406 39 of 69th

boundary layer. On the other hand, there is a large gradient of the NO_x concentration in the boundary layer, with the NO_x concentration 10 times more at the surface than at the top of the boundary layer. Therefore, with stratospheric ozone depletion, the net production of ozone increases in the lower boundary layer via the enhancement of peroxy radials due to the dominant role of NO_x , and decreases in the upper boundary layer via the loss of ozone itself due to the dominant role of water vapor.

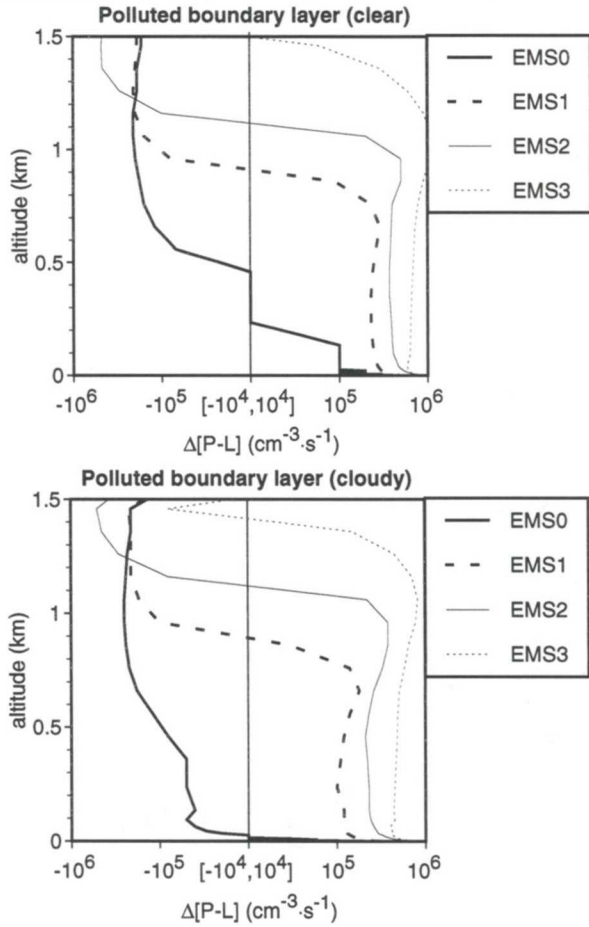


Figure 12 The difference in the local net production of ozone, $\Delta(P-L)$, due to stratospheric ozone depletion for the polluted boundary layer with various cases of NO_x and $NMHC_s$. a: Under the clear-sky condition (OZD2-REF0); b: Under a cloudy condition (D2L1-CDL1).

As shown in Figure 12a, among the four cases of the polluted regions, the order by which the net production of ozone in the boundary layer tends to increase with stratospheric ozone depletion is EMS3>EMS2>EMS1>EMS0. The NMHC_s limited region (EMS3) is the most favorable case, for which the increase in the net production of ozone occurs in the whole boundary layer (0-1.5 km); and the NO_x limited region (EMS0) is the least favorable one, for which the increase takes place only in the lower boundary layer up to the height of 0.4 km. The altitudes of turning point of the response and the corresponding NO_x concentrations are give in Table 6 as

40 of 69th

well. A higher NO_x condition is favorable for the increase in the net production of ozone with stratospheric ozone depletion. This can be seen by comparing the higher NO_x case (EMS2) with the lower NO_x case (EMS0), both of which are the same (higher) for NMHC $_s$. In addition to NO_x , NMHC $_s$ also plays an role in the response. The increase in the net production of ozone is larger for the lower NMHC $_s$ case (EMS3) than the higher NMHC $_s$ case (EMS2), both of which are the same (higher) for NO_x . The same effect of NMHC $_s$ can also seen by comparing the case EMS1 (lower) and the case EMS0 (higher) for the lower NO_x case, and the former (EMS1) is similar to the situation of Thompson et al. [1989], in which there is only ethane as NMHC $_s$. By comparing the case of the higher NO_x and higher NMHC $_s$ (EMS2) with the case of the lower NO_x and lowest NMHC $_s$ (EMS1), one can see that the role of NO_x still predominates over that of NMHC $_s$ in the response of the net production of ozone with stratospheric ozone depletion. Therefore, the lower NMHC $_s$ condition is more favorable for the increase in the net production of ozone in the polluted region when the NO_x levels are the same.

Figure 12b shows the change in the local net chemical production of ozone (up to the height of 1.5 km) with stratospheric ozone depletion for various cases of NO_x and $NMHC_s$ emissions under a cloudy condition (CDL1: τ =10 at 1-1.5 km). In all cases, the trends of the net production of ozone are similar to the situation as shown in Figure 12a. With clouds, the NO/NO_2 ratio decreases due to the decrease in J_NO_2 , which is infavored to the ozone production. Therefore in the lower boundary layer the net production of ozone increases under the cloudy condition than under the clear sky condition.

The variations in column integrated rate of the net ozone production due to a reduction in stratospheric ozone under the clear-sky (OZD2 relative to REF0) and a cloudy (D2L1 relative to CDL1) atmospheres are shown in Figure 13 for the polluted boundary layer with various cases of NO_x and NMHC_s conditions. In the boundary layer, the net production of ozone tends to decreases in the NO_x limited region (EMS0), but increases in the NMHC_s limited region (EMS3). Due to the coupled role of both NO_x and NMHC_s, the order of the case, by which the increase in the net production of ozone in the boundary layer is favored with stratospheric ozone depletion, is EMS3>EMS2>EMS1>EMS0. This trend is the same for both the clear sky and the cloudy atmosphere of this study. But the clear-sky condition is more favorable for the increase in the net production of ozone than the cloudy condition here.

TNO-report

TNO-MEP – R 96/406 41 of 69th

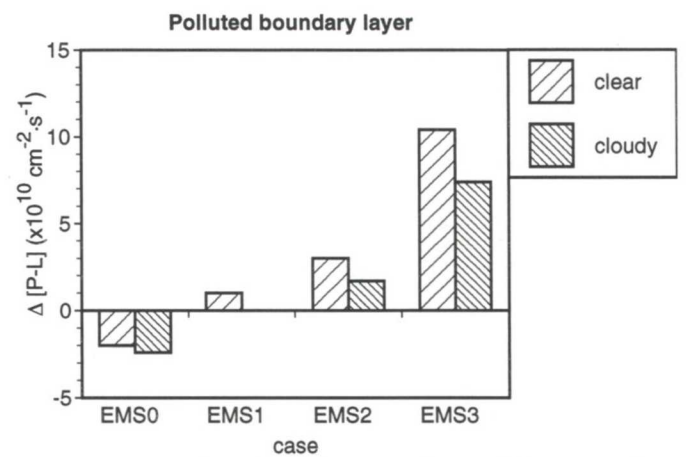


Figure 13 The difference in the column integrated rate of the net production of ozone, $\Delta(P-L)$, due to stratospherioc ozone depletion for the polluted boundary layer with various cases of NO_x and $NMHC_s$ under both the clear sky (OZD2-REF0) and a cloudy condition (D2L1-CDL1).

One thing to be mentioned is that the focus of this study is on the net production instead of the concentration of ozone. In addition to the local net production, in-situ ozone concentration also depends on the amount of ozone transported in and out of the region concerned. In the remote region, stratospheric ozone depletion will, most likely, cause a negative trend in the concentration of tropospheric ozone, because the net destruction of ozone increases in the whole troposphere over a large area there. In the polluted region, however, the trend in the concentration of ozone with stratospheric ozone depletion may not easily be seen because of the complicated situation there. First, while the net production of ozone in the whole or lower boundary layer increases with stratospheric ozone depletion, the net production decreases in the free troposphere and, even in some case, the upper boundary layer, leading to less amount of ozone transported form the free troposphere to the boundary layer and then down to the surface. Therefore, the ozone concentration may not increase or even decrease, since the increase in the net production in the lower boundary layer has to compensate the reduction of ozone transported from the free troposphere and/or the upper boundary layer. Second, the perturbation due to stratospheric ozone depletion is small relative to other effects, such as emissions and clouds, in the polluted region. So the effect of stratospheric ozone depletion may be shielded by other perturbations.

Summary

The response in the net production of ozone to stratospheric ozone depletion depends not only on the ambient condition of NO_x but also on that of $NMHC_s$ and water vapor. The direction of the response is determined dominately by the NO_x , and also affected secondly by the $NMHC_s$ in the polluted regions. The water vapor has a great effect on the magnitude of the response. In the upper free troposphere, the net produciton of ozone changes slightly with stratospheric ozone depletion due to the low concentration of water vapor there. In the lower free troposphere and the

boundary layer of the ocean and the clean continent, the net produciton of ozone decreases significanly due to both the low concentration of NO_x and the high concentration of water vapor. In the boundary layer of the polluted continent, the increase in the net production of ozone is more favored in the $NMHC_s$ limited region, and less or not favored in the NO_x limited region. Anyhow, the variation in the net production of ozone over the polluted regions with stratospheirc ozone depletion is small in a relative sense.

4.2.3 Effect of tropospheric pollution

Figure 14 shows the changes in the local net chemical production of ozone, i.e., $\Delta(P-L)$, due to tropopsheric pollutants, i.e., ozone (O_3) , sulfur dioxide (SO_2) and aerosols of this study, through the variations in the radiation. With comparison to stratospheric ozone depletion (Figure 10c), the responses of the net production of ozone with tropospheric pollution are opposite in direction, being larger in the lower boundary layer near the surface and smaller at the top of the boundary layer and above. This is because the changes in J_values due to tropospheric pollution occurs mostly in the lower troposphere, which can offset those due to stratospheric ozone depletion in the boundary layer (Figure 6). The effect of aerosols (PLA1) is most significant among the pollutants of this study, as both $J_{-}O_{3}(^{1}D)$ and $J_{-}NO_{2}$ decreases with the aerosols and the role of $J_{-}NO_{2}$ predomintes over that of $J_{-}O_{3}(^{1}D)$ in the chemical budget of ozone in the polluted boundary layer.

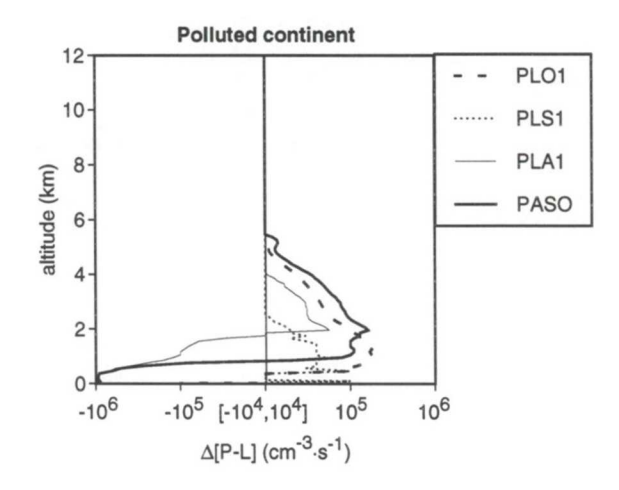


Figure 14 The difference in the local net production of ozone, $\Delta(P-L)$, due to tropospheric pollution through radiation variations for the polluted continent with respect to the clear-sky condition (REF0).

The variations in column integrated rate of the net ozone production due to tropospheric pollution are shown in Figure 15. One can see that there is a large decrease in the boundary layer mainly due to the effect of the aerosols (PLA1), and a small increase in the free troposphere mainly due to the effect of ozone (O₃) (PLO1). The effect of sulfur dioxide (SO₂) (PLS1) is very small.

TNO-MEP - R 96/406 43 of 69th

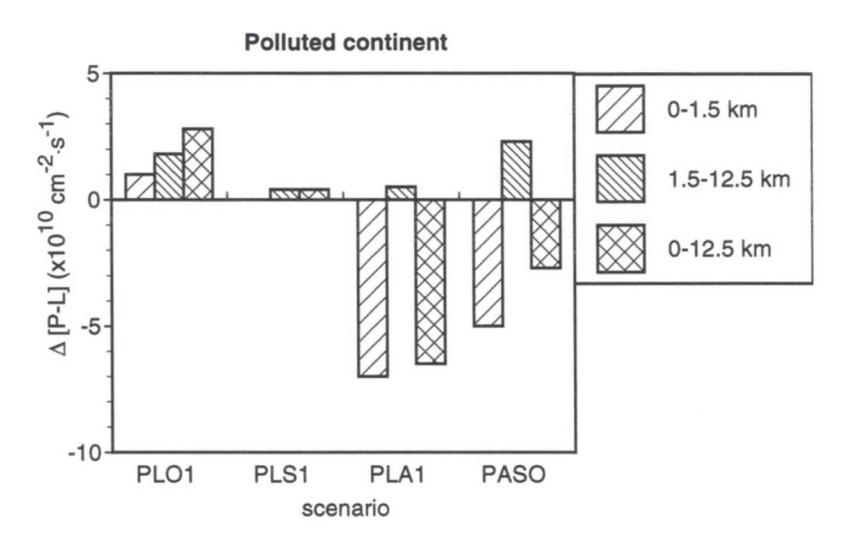


Figure 15 The difference in the column integrated rate of the net production of ozone, $\Delta(P-L)$, due to tropospheric pollution through radiation variations for the boundary layer, the free troposphere and the whole troposphere over the polluted continent with respect to the clear-sky condition (REF0).

4.3 Chemical Reactions

The chemistry on the production and destruction of ozone in the troposphere has been discussed in Section 2. Generally, the photochemical rate of ozone production is given by

$$P = \lceil NO \rceil \cdot (k_{11} \cdot \lceil HO_2 \rceil + \sum k_{14a} \cdot \lceil RO_2 \rceil) \tag{F6}$$

and the photochemical rate of ozone destruction is expressed approximately by

$$L = [O_3] \cdot (J_O_3(^1D),_{eff} + k_4 \cdot [HO_2] + k_5 \cdot [OH])$$
 (F7)

In the continental boundary layer, over the polluted region in particular, the loss processes of odd oxygen via (R22) and (R29) followed by the heterogeneous removal of nitric acid or aerosol nitrate are also considerable for the photochemical rate of ozone destruction (k₂₂[OH][NO₂][M]+k₂₉[N₂O₅][H₂O_{1q}]), which are included in (F7) for the continental case. Due to the rapid cycle of PAN in (R23), the production and loss of ozone through (R23) are not included in (F6) and (F7), respectively. Other processes, e.g., potential losses occurring in cloud droplets, are not considered in this study.

44 of 69th

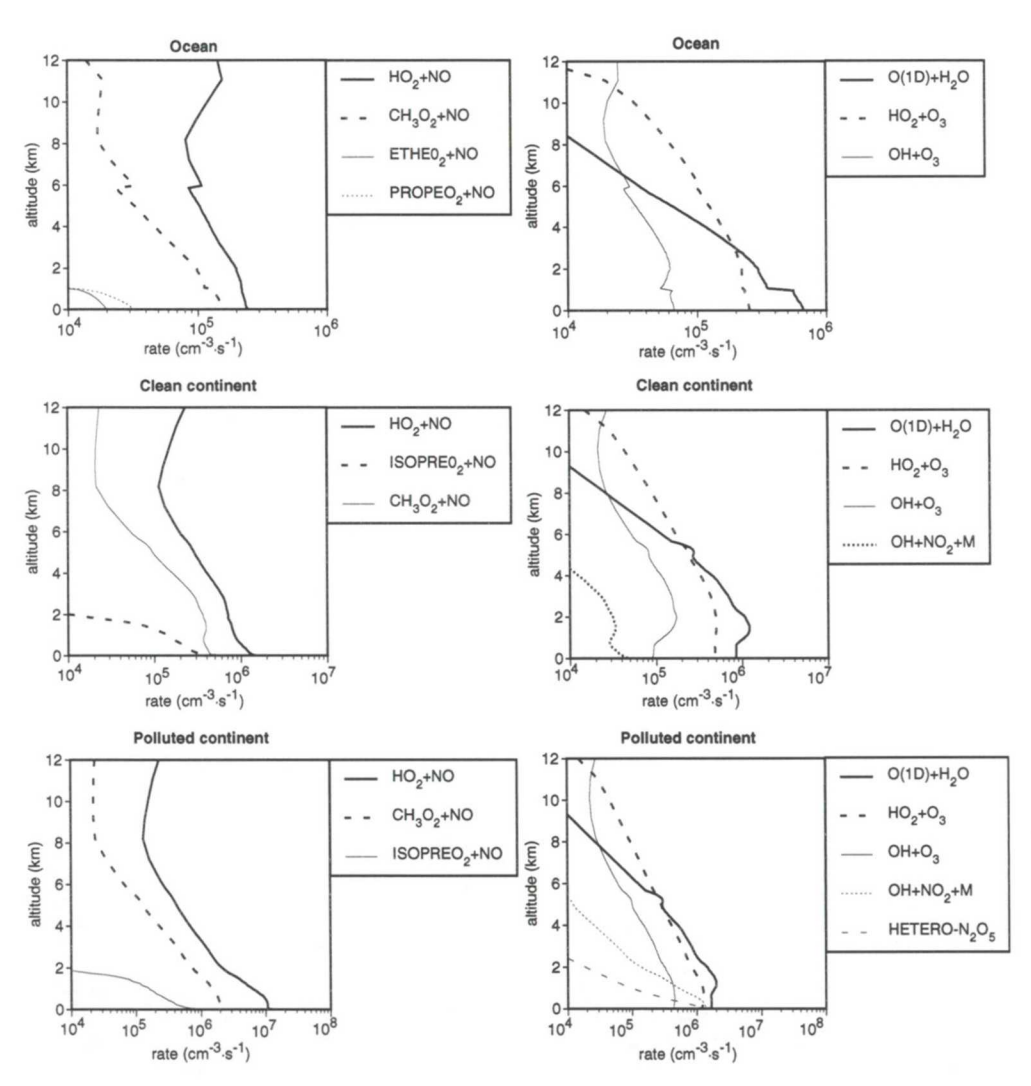


Figure 16a
The local rates of the chemical reactions
that are important for the ozone production
in the troposphere over the ocean, the clean
continent and the polluted continent under
the clear-sky condition (REF0)

Figure 16b
Same as Figure 16a, but for the ozone destruction.

The main chemical reactions that contribute to the rates of production and destruction of tropospheric ozone for the ocean, clean continent and polluted continent are given in Figure 16a and Figure 16b, respectively. For the ozone production (Figure 16a), reaction HO₂+NO (R11) is dominant in all regions, and the followed is CH₃O₂+NO. The peroxy radicals ETHEO₂ (HOCH₂CH₂O₂) and PROPEO₂ (HOCH₂CHO₂CH₃) in the oceanic boundary layer, and ISOPREO₂ (ISOPRENE-RO₂) in the continental boundary layer, also make a small contribution to the ozone production by reaction with NO. For the ozone destruction (Figure 16b), the photolysis of O₃ followed by the reaction with water vapor (R2), i.e., the effective photolysis of O₃, is dominant in the lower troposphere, while reaction HO₂+O₃ (R4) is dominant in the upper troposphere. Reaction HO+O₃ (R5) also plays an role

TNO-MEP - R 96/406 45 of 69th

in the destruction of ozone, but only becomes important near the tropopause. In the continental boundary layer, reaction OH+NO₂+M (R22) makes a small contribution to the ozone destruction. The contribution of reactions OH+NO₂+M (R22) and N₂O₅+H₂O_{lq} (R29) to the ozone destruction is considerable only at the surface of the polluted region.

4.3.1 Effect of clouds

The relative contributions of selected chemical reactions to the variation in the net production of ozone with the low clouds (CDL1: τ =10 at 1-1.5 km) relative to the clear sky (REF0) are shown in Figure 17. One can see that O(¹D)+H₂O (R2) and HO₂+NO (R11) are the most important reactions for the response of the chemical budget of ozone in the troposphere to the perturbation of the clouds. The change in the rate of reaction $O(^{1}D)+H_{2}O(R2)$ is caused by that of $J O_{3}(^{1}D)_{seff}$ (Figure 4), and the change in the rate of reaction HO₂+NO (R11) mainly by that of J NO₂ (Figure 3a) which converts more NO₂ back to NO. The changes in the net production of ozone (Figure 8) can be explained simply by the changes in rates of reaction O(¹D)+H₂O (R2) and HO₂+NO (R11). Above the clouds, the increase in the rate of HO₂+NO (R11), with the surplus of a small increase in the rate of CH₃O₂+NO, predominates over the decrease in the rate of O(¹D)+H₂O (R2), leading to the increase in the net production of ozone. In the clouds, the decrease in the rate of $O(^{1}D)+H_{2}O$ (R2) is significant, while the change in the rate of $HO_{2}+NO$ (R11) is relatively small, so that there is a large decrease in the net production of ozone. Below the clouds over the ocean, the changes in the rates of these two reactions are comparable, and thus the change in the net production of ozone is very small. Below the clouds over the continent, both the decrease in the rate of HO₂+NO (R11) and the increase in the rate of O(¹D)+H₂O (R2) cause the decrease in the net production of ozone.

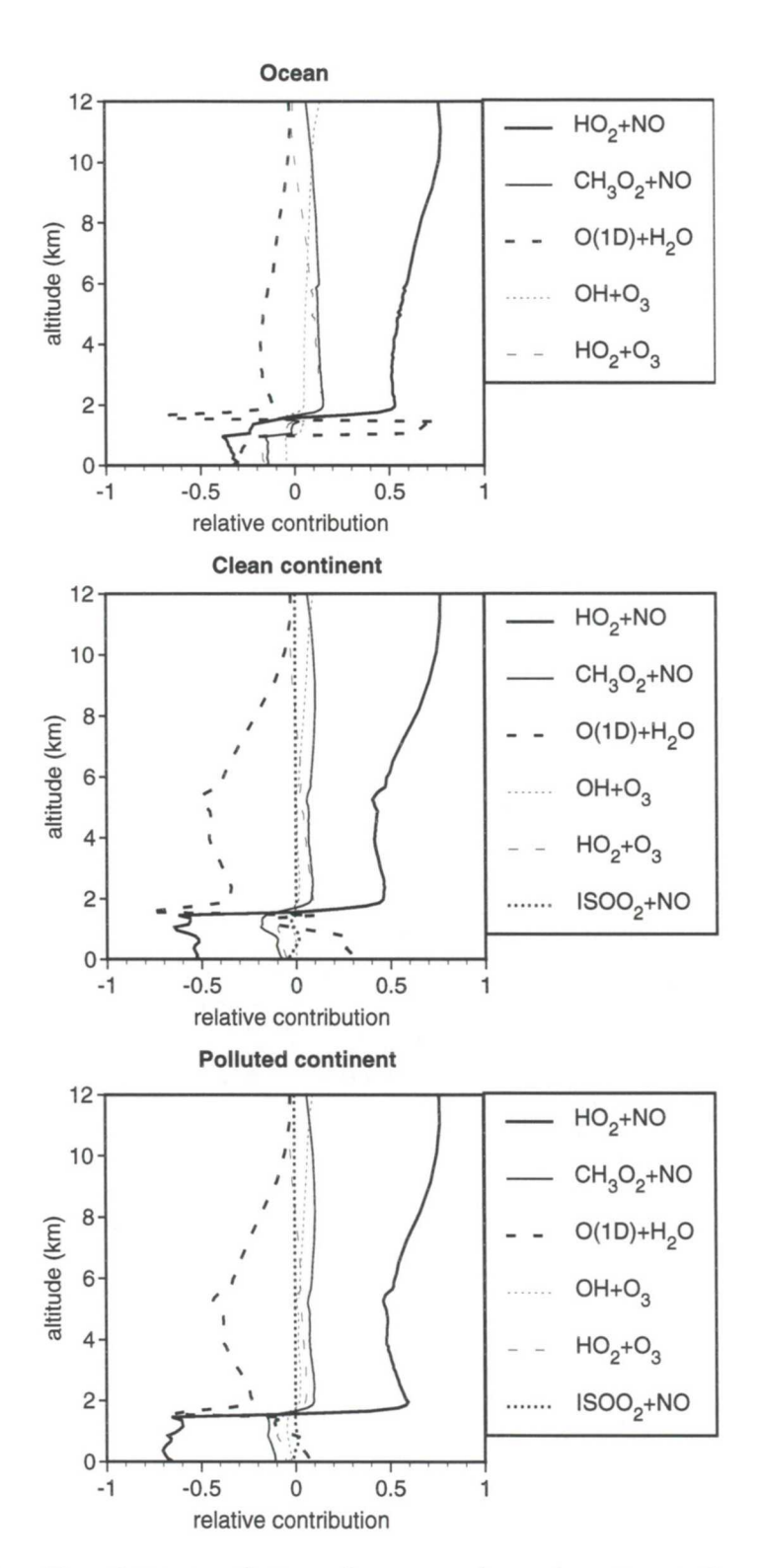


Figure 17 The relative contributions of important chemical reactions to the variation in the net production of ozone, $\Delta rate/\sum |\Delta rate_i|$, due to the low clouds (CDL1) with respect to the clear-sky condition (REF0).

TNO-MEP - R 96/406 47 of 69th

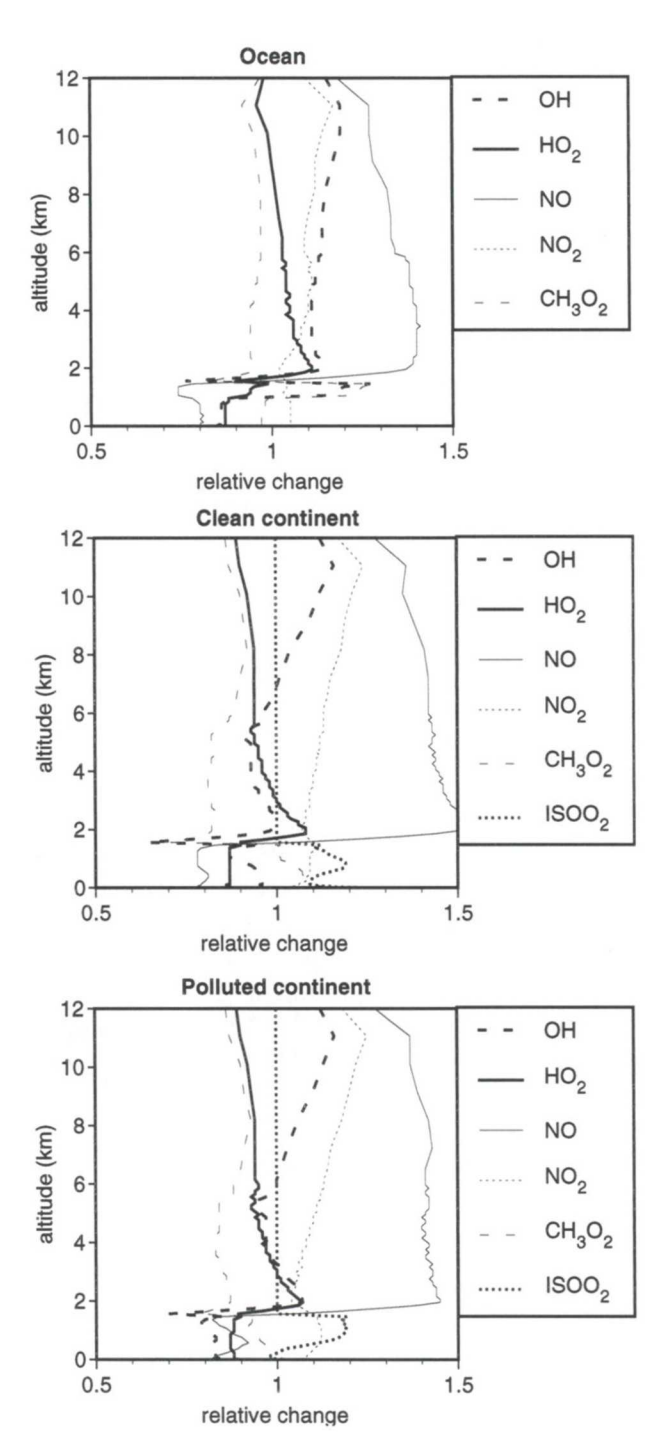


Figure 18 The changes in the concentrations of some species due to the low clouds (CDL1) relative to the clear-sky condition (REF0).

Figure 18 shows the changes in the concentrations of some species with the low clouds (CDL1: τ =10 at 1-1.5 km). Over all regions, the concentration of NO is increased above the clouds and decreased below the clouds, as same as the trend of J_NO₂. The effective photolysis of ozone is the main source of OH, and the concentration of OH changes significantly with the variation in J_O₃(1 D),_{eff}. The larg-

est change in the OH concentration in the clouds reflects the most pronounced variation in the rate of reaction $O(^1D)+H_2O$ (R2) occurring there. However, the change in the OH concentration with the clouds is not always predominated by the effective photolysis of O_3 , since the change in the NO concentration due to the photolysis of NO_2 may also causes the change in the OH concentration profoundly through reaction HO_2+NO (R11) when NO_x is available. For example, above the clouds over the ocean, OH is increased to a small extent, since the increase in reaction HO_2+NO (R11) is larger than the decrease in reaction $O(^1D)+H_2O$ (R2); while below the clouds over the continent, OH is decreased, since the decrease in reaction HO_2+NO (R11) is larger than the increase in reaction $O(^1D)+H_2O$ (R2). Over all regions, the increase of OH and the decrease of HO_2 in the upper troposphere, where the water vapor concentration is low, can be explained by the increase of reaction HO_2+NO (R11) with the increase in J_NO_2 .

OH can be produced, e.g., by the reaction of HO₂ with O₃ (R4) or NO (R11); and in turn, HO₂ can be converted from OH, e.g., in the oxidation of CO (R9 and R10) and hydrocarbons (R12 through R15). However, these reactions are not the ultimate sources of hydrogen radicals HO_x (= OH + HO₂), because OH and HO₂ are merely recycled. In the clouds over all regions, there is also a maximum for the concentration of HO₂ in coincidence with that of OH for each region, since a great amount of OH is converted to HO2 when OH itself increases significantly with its source, i.e., the effective photolysis of ozone. In the lower troposphere above the clouds of the continent, even though the increased reaction HO₂+NO (R11) can convert more HO₂ to OH, the concentration of OH as well as HO₂ is still decreased due to the decrease in the effective photolysis of ozone. However, the effective photolysis of ozone, is not a unique source of HO_x. In the lower troposphere above the clouds of the ocean, the concentrations of both OH and HO₂ are increased to a small extent, while the effective photolysis of O₃ is decreased; and the vice verse in the boundary layer below the clouds of the continent. Therefore, in addition to ozone, the photolysis of other species may also be responsible for the changes in HO_x and thus the chemical budget of ozone in the troposphere.

Figure 19 shows the changes in the photolysis rates of selected species due to the low clouds (CDL1: τ =10 at 1-1.5 km) relative to the clear sky condition (REF0). In addition to the effective photolysis of O₃, OH can also be produced directly by the photodissociation of H₂O₂ and CH₃OOH. The photodissociation of HCHO (through path A, i.e., \rightarrow H+CHO) and CH₃OOH will lead to the formation of HO₂. As shown in the figure, the photolysis of HCHO is most sensitive to the perturbation among other species except O₃. The increase in the concentrations of HO_x (= OH + HO₂) in the lower troposphere above the clouds of the ocean and the decrease in the boundary layer below the clouds of the continent, can be explained by the variation in the photolysis rates of HCHO, H₂O₂ and CH₃OOH there. In the lower troposphere above the clouds of the ocean, the photolysis rates of HCHO, H₂O₂ and CH₃OOH increase, and in the boundary layer below the clouds of the continent, the photolysis rates of HCHO, H₂O₂ and CH₃OOH decrease, leading to HO_x to respond

TNO-MEP - R 96/406 49 of 69th

in contrast to the variation of the effective photolysis rates of O_3 . In the upper troposphere over the continent, the small decrease in the photolysis rates of H_2O_2 is caused by the decrease in the abundance of H_2O_2 itself, as the concentration of HO_2 , which can combine to form H_2O_2 , is decreased above the clouds. Therefore, while the photolysis of the species provides the sources of the radicals, in feedback, the concentrations of these and other species also depends on ambient abundance of radicals, OH and HO_2 . In addition to HCHO, H_2O_2 and CH_3OOH , the photolysis of other species, such as HNO_3 , HNO_2 , CH_3CHO and methylglyoxal (CH_3COCHO) is not so important, which merely contributes to the formation of HO_x to a smaller extent near the surface.

The changes in the concentrations of NO₂ and CH₃O₂ (and ISOO₂ for continent) are also shown in Figure 18. The changes in the NO₂ concentration may be determined by the combined effects of the photolysis of NO2, reactions with varied OH and HO₂, and the photolysis of other nitrogen species such as HNO₃, HNO₂ and NO₃. The increase in the concentration of NO₂ in the lower boundary layer below the clouds over all regions can be explained by the decrease in the photolysis rates of NO₂, (R6), and by the decrease in OH and HO₂, which can react with NO₂ to form HNO₃ and HNO₄, respectively. This story can not be applied to the free troposphere above the clouds where the concentrations of both NO and NO₂ i.e., NO_x, are increased with the increase in the photolysis rates of NO₂ and/or HO_x. This is because the photolysis of NO_x reservoirs, such as HNO₃, HNO₂ and NO₃, increase above the clouds and leads to more NO_x. The change in the concentration of CH₃O₂ appears to depend on NO more than OH or HO₂, except for the polluted boundary layer below the clouds, where the concentration of CH₃O₂ decreases with the decrease in the concentrations of OH and HO2. Anyhow, the changes in chemical reactions for ozone production via (R11) and (R14a) are predominated by the variations in the concentration of NO with the clouds of this situation.

Summary

The reaction $O(^1D)+H_2O$ (R2) and HO_2+NO (R11) are the most important reactions for the response of the chemical budget of ozone in the troposphere to the perturbation of the clouds. The rate of reaction $O(^1D)+H_2O$ (R2), which contributes to the chemical destruction of ozone, changes with $J_2O_3(^1D)_{\text{eff}}$. The rate of reaction HO_2+NO (R11), which contributes to the chemical production of ozone, changes mainly with J_2NO_2 . With the clouds, the concentration of OH can be changed not only due to the variation in its source, mainly the effective photolysis of ozone, but also due to the conversion among HO_x , especially via the reaction HO_2+NO (R11).

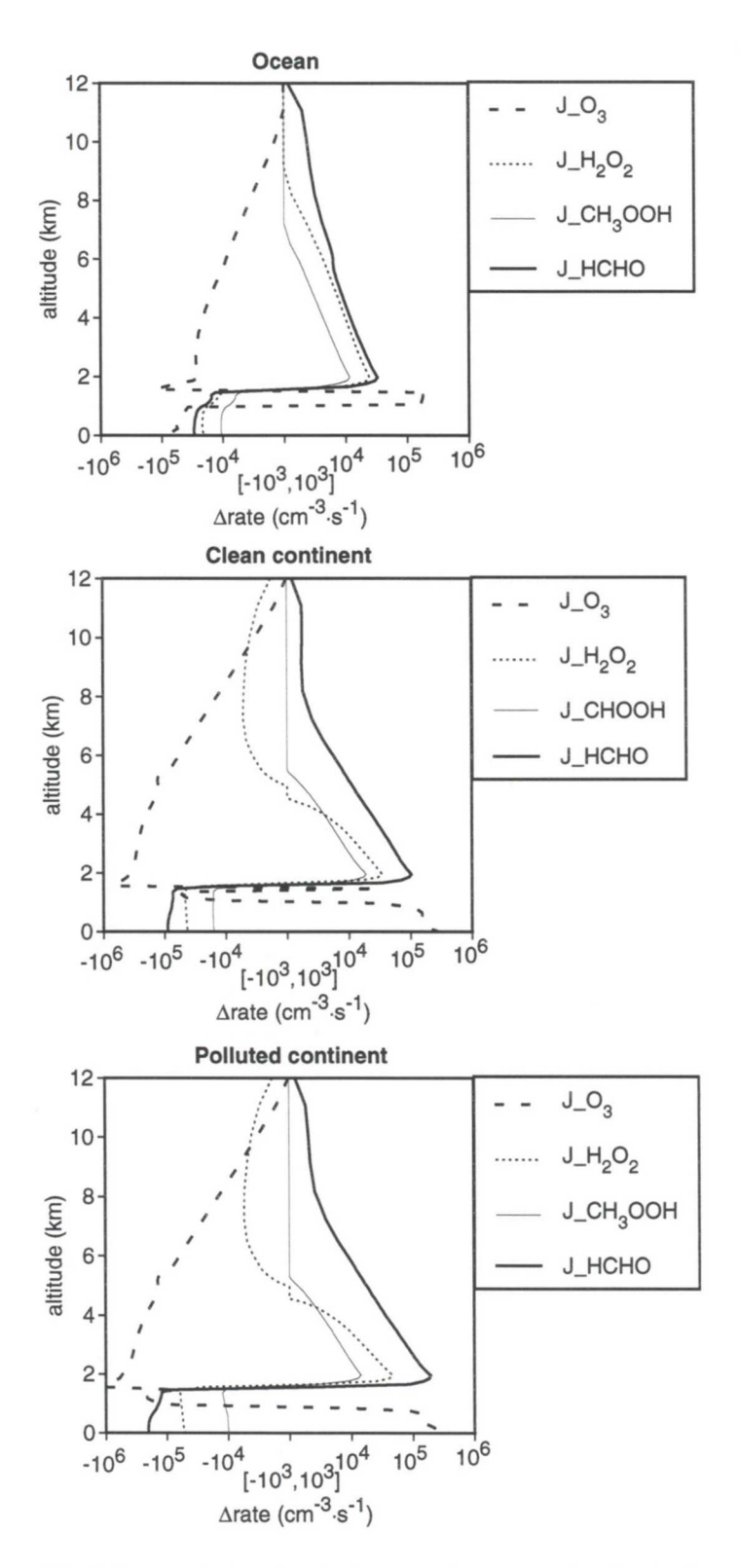


Figure 19 The difference in the photolysis rates of some species, Δ rate, due to the low clouds (CDL1) with respect to the clear-sky condition (REF0).

TNO-MEP - R 96/406 51 of 69th

4.3.2 Effect of stratospheric ozone depletion

The relative contributions of selected chemical reactions to the variation in the net production of ozone with stratospheric ozone depletion (OZD2: a reduction by 10% relative to REF0) are shown in Figure 20. In this case, $O(^1D)+H_2O$ (R2) is the most important reaction for the response of the chemical budget of tropospheric ozone to the perturbation over all regions, while the change in the rate of reaction HO_2+NO (R11) becomes comparable only in the lower boundary layer over the polluted region. The change in the rate of reaction HO_2+NO (R11) is dominant in the upper troposphere, as the effective photolysis of ozone is limited due to the low water vapor. However, the absolute changes there are very small and, thereby, the changes in the net production of ozone are negligible in the upper troposphere. The significant increase in the effective photolysis of ozone, (R1) followed by (R2), leads to the increase (or decrease) in the net destruction (or production) of ozone in the lower troposphere over all regions, except in the lower polluted boundary layer, where there is an increase in the net production of ozone due mainly to the increases in the rate of reaction HO_2+NO (R11) (Figure 10).

The changes in the concentrations of selected species in the troposphere with stratospheric ozone depletion (OZD2: a reduction by 10% relative to REF0) are shown Figure 21. First of all, one can see that the changes in the concentrations of these species are small relative to those due to the perturbation of the clouds (Figure 18). The concentration of OH increases most significantly in the lower troposphere over all regions, due to the increase in $J_{O_3}(^1D)_{\text{reff}}$. The concentrations of HO_2 and CH_3O_2 over all regions, and $ISOO_2$ in the lower boundary layer of the continent, are also increased mainly through the oxidation of CO (R9 and R10) and hydrocarbons (R12 through R15) by OH. The increases in these peroxy radicals contribute to the increase in the chemical ozone production with stratospheric ozone depletion when the NO_x is available.

The stratospheric ozone depletion has little effect on the photolysis of NO_2 and, thereby, the change in the concentrations of NO and NO_2 due to the conversion between these two species is very small. In the boundary layer, there are small decreases in the concentration of NO_x (= $NO + NO_2$) due to the increased rates of its reactions with OH and HO_2 , which form the reservoirs, e.g., HNO_3 and HNO_4 . The response in the photolysis rates of the NO_x reservoirs as well as other compounds, is not as sensitive as that of O_3 . Figure 22 shows the changes in the photolysis rates.

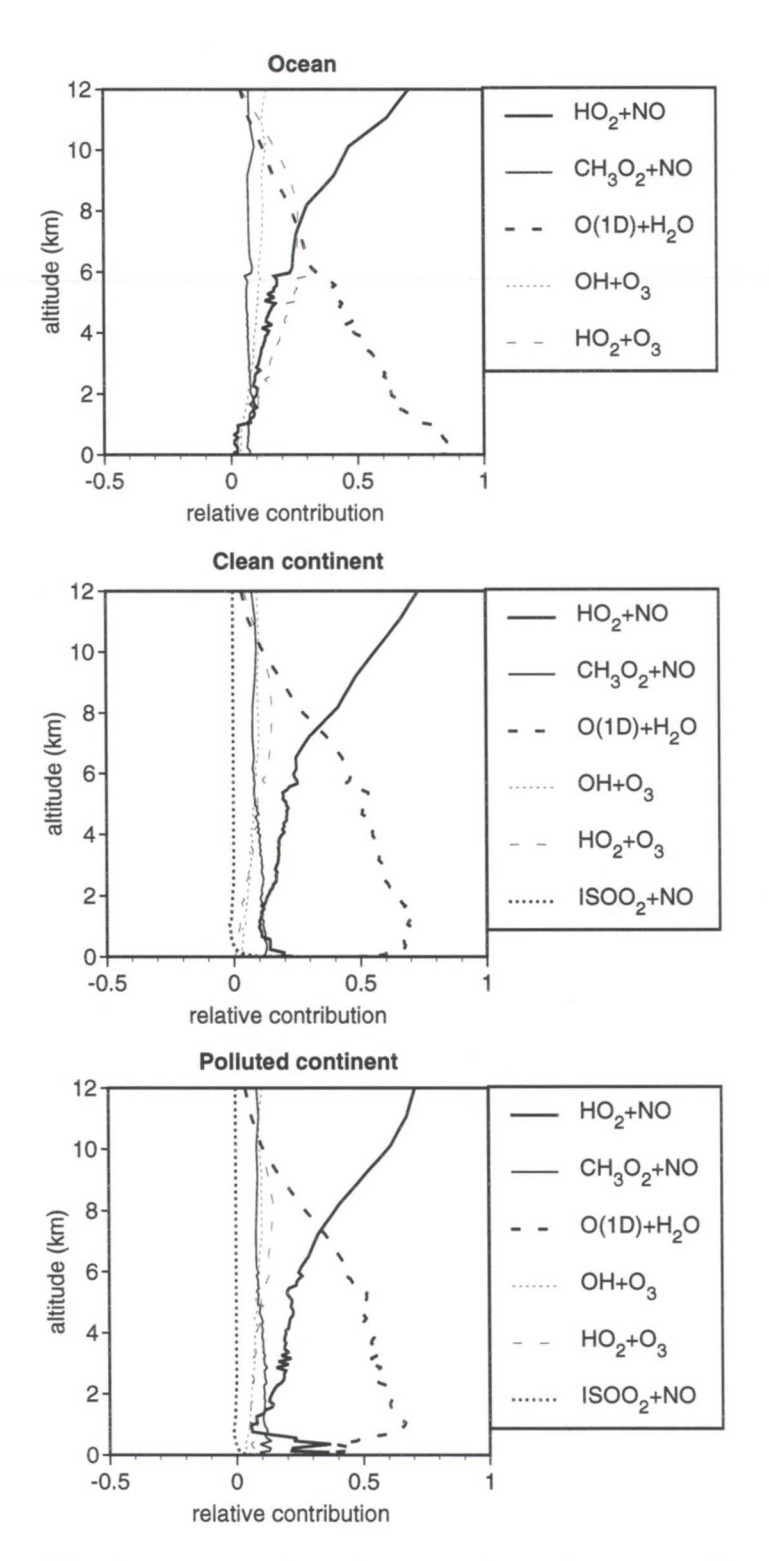


Figure 20 The relative contributions of important chemical reactions to the variation in the net production of ozone, $\Delta rate_i / \sum |\Delta rate_i|$, due to stratospheric ozone depletion (OZD2) with respect to the clear-sky condition (REF0).

TNO-MEP - R 96/406 53 of 69th

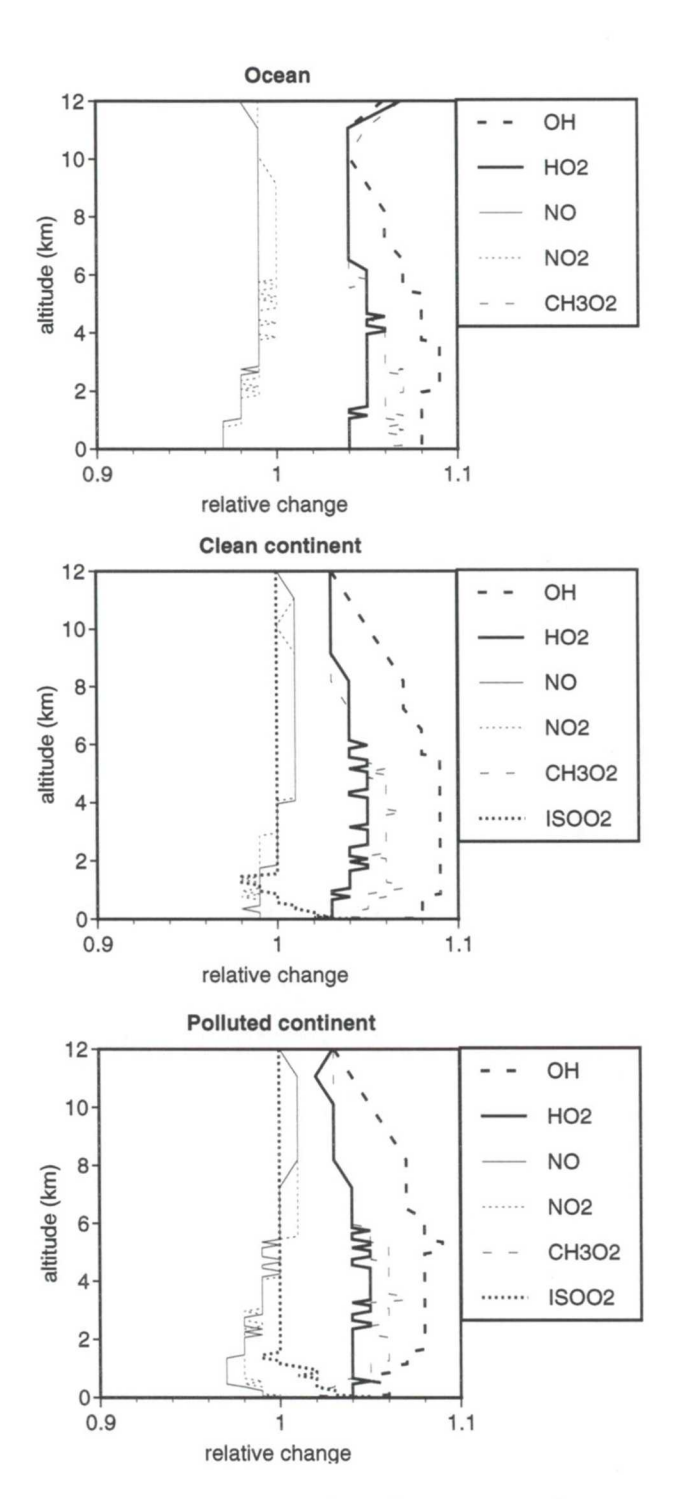


Figure 21 The changes in the concentrations of some species due to stratospheric ozone depletion (OZD2) relative to the clear-sky condition (REF0).

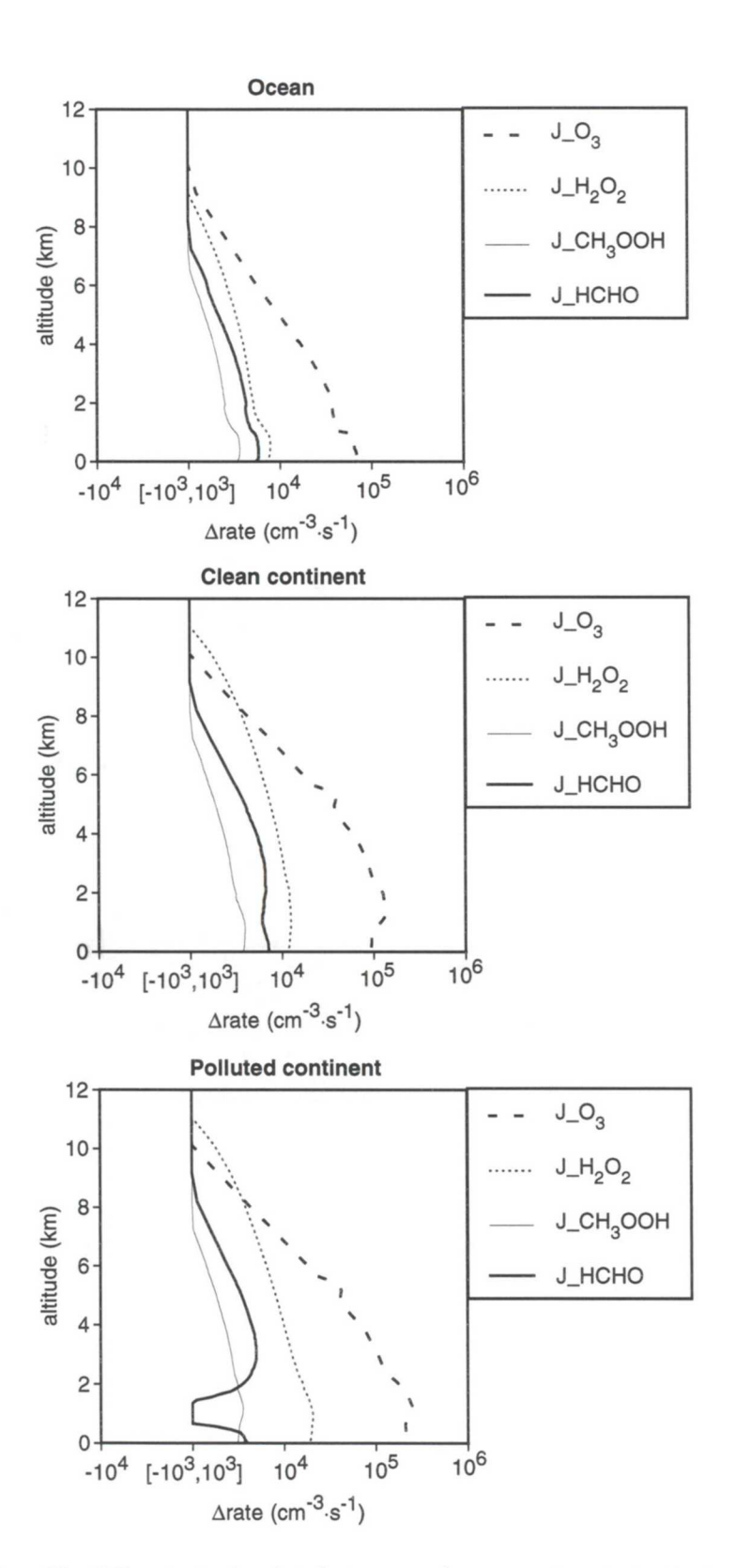


Figure 22 The difference in the photolysis rates of some species, Δ rate, due to stratospheric ozone depletion (OZD2) with respect to the clear-sky condition (REF0).

TNO-MEP - R 96/406 55 of 69th

of selected species due to stratospheric ozone depletion. The photolysis of H_2O_2 is most sensitive to the perturbation among other species except O_3 , and even predominates over the effective photolysis of O_3 in the upper troposphere near the tropopause. The increase in photolysis rates of these species may also contribute to the increase in the concentrations of HO_x (= $OH + HO_2$) to a smaller extent.

Polluted boundary layer

The changes in the rates of selected chemical reactions with stratospheric ozone depletion (OZD2: a reduction by 10% relative to REF0) are shown in Figure 23 for for various conditions of NO_x, NMHC_s (Table 5). While reaction O(¹D)+H₂O (R2) increases pronouncedly at all altitudes of the boundary layer, reaction HO₂+NO (R11) changes slightly in the upper boundary layer and increases significantly in the lower boundary layer. The increase in the rate of reaction HO₂+NO (R11) can be so large to predominate over that of reaction O(¹D)+H₂O (R2). The altitude at which the steep increase in the rate of reaction HO₂+NO (R11) occurs is in good agreement with the tuning-point of the response of the net production of ozone to stratospheric ozone depletion for each case (Table 6). The small increases in the rates of reaction CH₃O₂+NO and ISOO₂+NO also makes a contribution to the increase in the ozone production. As shown in Figure 23a, for example, even though the increase in the rate of reaction HO₂+NO (R11) is not large enough to overcome that of reaction O(¹D)+H₂O (R2), the net production of ozone still increases up to the height of about 0.4 km, due to the surplus of the increase in the rate of reaction CH₃O₂+NO.

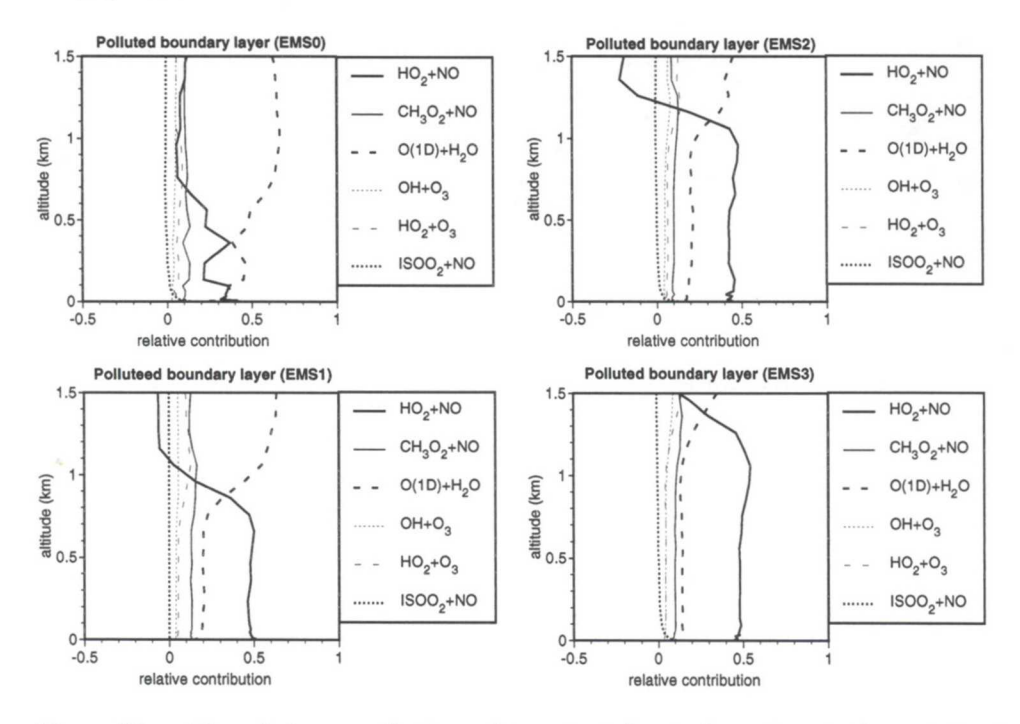


Figure 23 The relative contributions of important chemical reactions to the variation in the net production of ozone, $\Delta rate_i / \Delta rate_i$, due to stratospheric ozone depletion (OZD2) for the polluted boundary layer with various cases of NO_x and $NMHC_s$ with respect to the clear-sky condition (REF0).

The changes in the concentrations of selected species with stratospheric ozone depletion are shown in Figure 24 for each case. The role of NMHC_s in the response can been seen by comparing the higher NMHC_s case (EMS0 for the lower NO_x or EMS2 for the higher NO_x) with the lower NMHC_s case (EMS1 for the lower NO_x and EMS3 for the higher NO_x) at the same condition of NO_x. The enhancement of HO₂ is greater for the lower NMHC_s case (EMS1 or EMS3) than for the higher NMHC_s case (EMS0 or EMS2). For the lower NMHC_s case (EMS1 or EMS3), the increase in the concentration of HO₂ is even larger than that of OH at the same case. This is because that more OH will react with CO and CH₄ for the lower NMHC_s case, and less OH will react with CO and CH₄ for the higher NMHC_s case, due to the competition of NMHC_s with CO and CH₄. The reaction of OH with CO via (R9) and (R10) will produce HO₂ efficiently. The reaction of OH with CH₄ will produce HO₂ and formaldehyde (HCHO) through (R12) to (R15), and HO₂ can be produced further from HCHO by the reaction with OH via (R16) and/or by the photolysis of itself via (R17a). The reaction of OH with NMHC_s will produce HO₂ and other aldehydes (R>C1) or ketone instead of HCHO through (R12) to (R15), and these aldehydes or ketone may not produce HO2 as efficiently as HCHO due to the formation of other peroxy radicals or intermediate products.

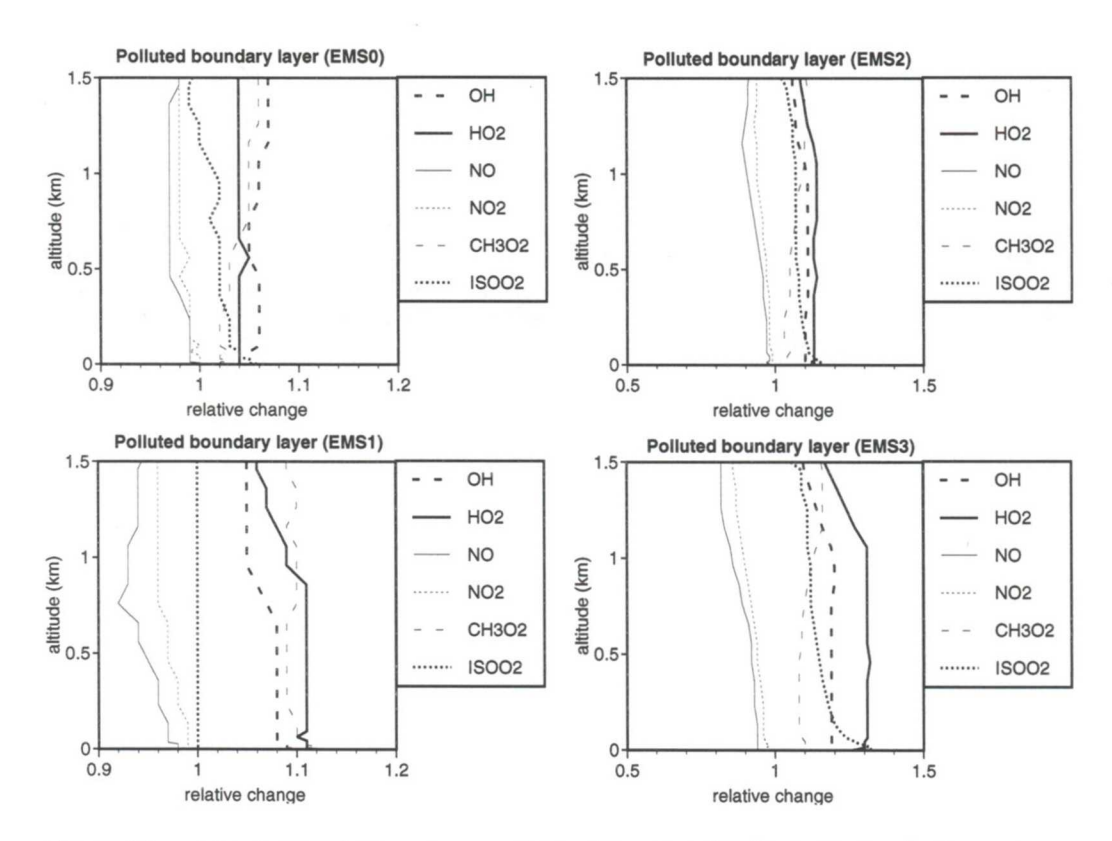


Figure 24 The changes in the concentrations of some species due to stratospheric ozone depletion (OZD2) for the polluted boundary layer with various cases of NO_x and NMHC_s relative to the clear-sky condition (REF0).

TNO-MEP - R 96/406 57 of 69th

Figure 25 shows the changes in the photolysis rates of selected species with stratospheric ozone depletion at various NO_x and NMHC_s conditions. One can see that, with comparison to other species, the changes in the photolysis rate of HCHO (\rightarrow H+CHO) are quite different between the lower NMHC_s case and the higher NMHC_s case, i.e., EMS0 with EMS2 or EMS3 with EMS4. This difference due to HCHO leads to the different responses of HO₂ (Figure 24) and thus those of reaction HO₂+NO (Figure 23). The reaction HO₂+NO (R11) is more efficient than the reaction RO₂+NO (R14a) in the production of ozone on the basis of per peroxy radical unit. This can be shown by comparing the ozone equivalent units of HO₂ and RO₂ in the conversion of NO to NO₂, i.e., the ratios of the rate constants $k(NO+O_3)/k(NO+HO_2)$ and $k(NO+O_3)/k(NO+RO_2)$ [Parrish et al., 1986]. Table 7 gives the related rate constants and ozone equivalent units of HO2 and RO2 at temperature of 285 K and 295 K, respectively. All the reaction rate constants of organic peroxy radicals with NO are assumed to the same as that of CH₃O₂ in the model. The values in Table 7 indicates that less amount of HO₂ than RO₂ is needed to convert same quantity of NO to NO₂. While HO₂ and RO₂ are much more efficient in the oxidation of NO than O₃ on the basis of per molecule, reaction NO+O₃ (R8) is still important and dominant in the photostationary state of NO, NO₂ and O₃ because of the greater amount of O_3 .

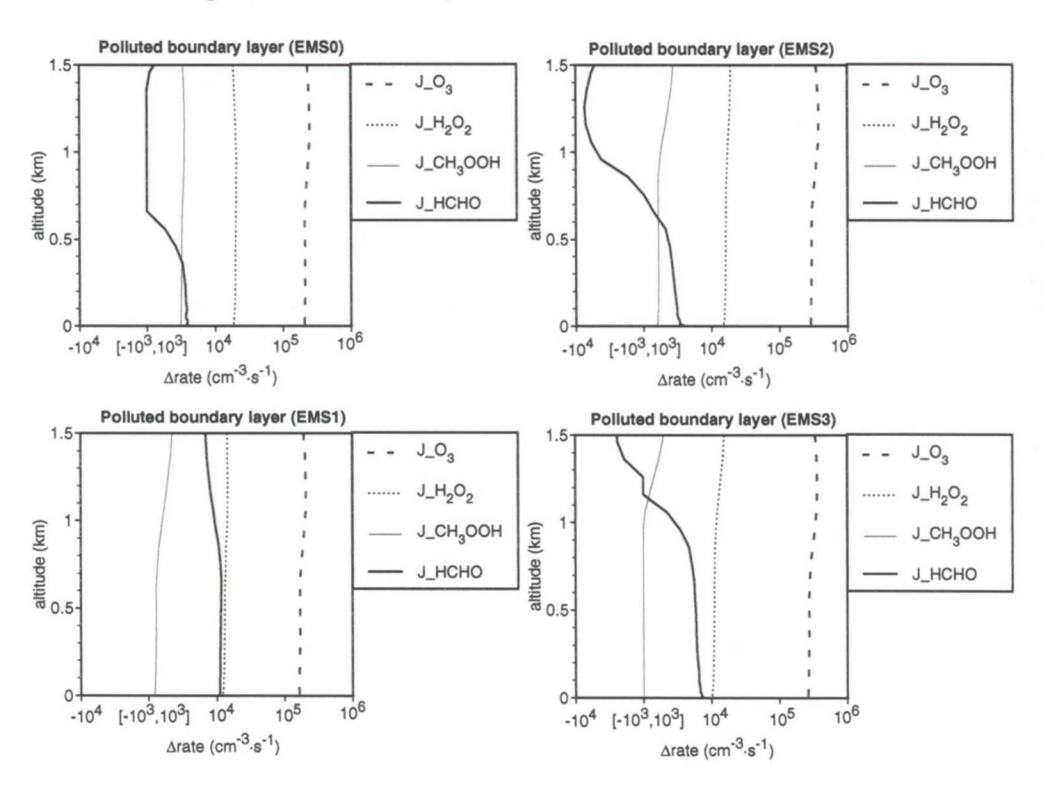


Figure 25 The difference in the photolysis rates of some species, Δ rate, due to stratospheric ozone depletion (OZD2) for the polluted boundary layer with various cases of NO_x and $NMHC_s$ with respect to the clear-sky condition (REF0).

Table 7 The ozone equivalent units of peroxy radicals in the conversion of NO to NO₂.

Ta	k(NO+O ₃) ^b	k(NO+HO ₂) ^D	k(NO+RO ₂) ^b	HO ₂ ^c	RO₂ ^c
285	1.5×10 ⁻¹⁴	8.6×10 ⁻¹²	7.9×10 ⁻¹²	1.7	1.9
295	1.7×10 ⁻¹⁴	8.3×10 ⁻¹²	7.7×10^{-12}	2.1	2.3

a temperature, K;

The changes in the rates of most important chemical reaction rates in the polluted boundary layer with various NO_x and NMHC_s emissions are discussed above for the clear sky condition (OZD2 relative to REF0). Under a cloudy condition (CDL1: τ =10 at 1-1.5 km), the effective photolysis rate of ozone increases due to the increase in water vapor below the low cloud (Figure 4b), whereas the photolysis rates of the other species decrease with the clouds. Therefore, with stratospheric ozone depletion, the enhancement of OH will be more favored below the low clouds than in the clear sky with comparison to HO₂. Figure 26 shows the changes in the ratio of HO₂/OH at various NO_x and NMHC_s cases under the conditions of the clear sky (OZD2/REF0) and the clouds (D2L1/CDL1), respectively. Except for the NO_x limited region (EMS0: the lower NO_x and higher NMHC_s case), the ratio of HO₂/OH is increased with stratospheric ozone depletion, and this increase is more under the clear sky condition than under the cloudy condition for the same case. The responses of the chemical reactions to stratospheric ozone depletion under the cloudy condition are similar to those under the clear-sky condition, except that the reaction O(¹D)+H₂O (R2) increases more with stratospheric ozone depletion below the low clouds than in the clear sky. Sofar, it can be seen that, in addition to NO_x and NMHC_s, the water vapor also plays a role in the perturbation due to stratospheric ozone depletion.

b rate constants, cm³·s⁻¹;

c ozone equivalent units in the conversion of NO to NO₂, pptv for 1 ppbv ozone equivalent units.

TNO-MEP - R 96/406 59 of 69th

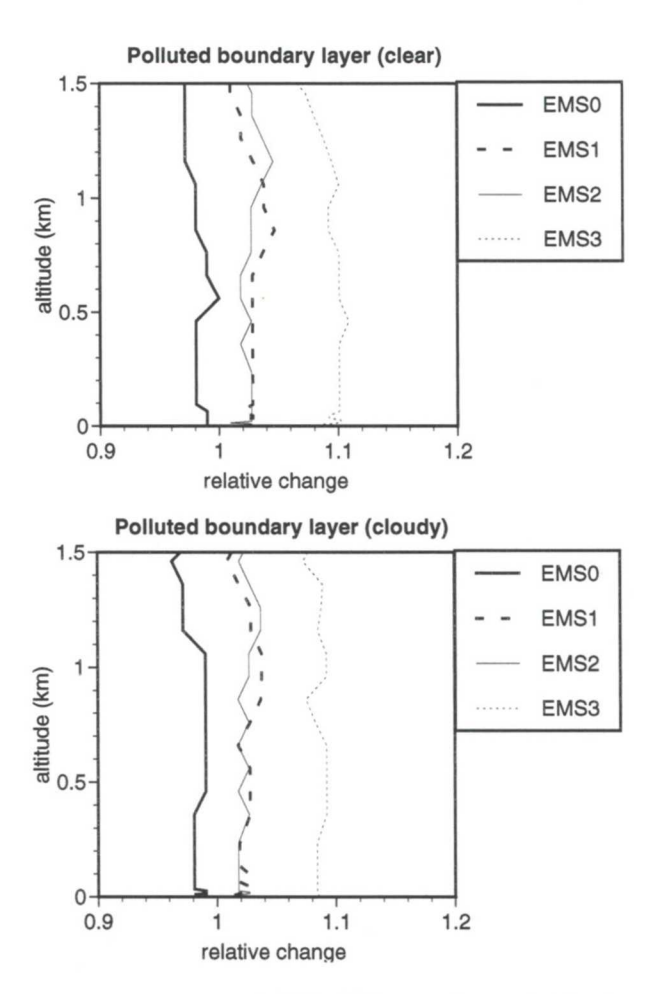


Figure 26 The relative changes in the HO₂/OH ratio due to stratospherioc ozone depletion for the polluted boundary layer with various cases of NO_x and NMHC_s.

a: Under the clear-sky condition (OZD2/REF0); b: Under a cloudy condition (D2L1/CDL1).

Summary

The reaction $O(^1D)+H_2O$ (R3) is the most important reaction for the response of the chemical budget of ozone in the troposphere to the perturbation of stratospheric ozone depletion. The increase in the rate of reaction $O(^1D)+H_2O$ (R2), due to the increase in $J_O_3(^1D)$,_{eff}, leads to the decrease in the net production of ozone over almost all regions, except for the lower boundary layer of the polluted region. In the polluted boundary layer where the NO_x is high, the increase in the rate of reaction HO_2+NO (R11), due to the enhancement of HO_2 , is also important and may be larger than that of reaction $O(^1D)+H_2O$ (R2), leading to the increase in the net production of ozone. The enhancement of HO_2 is more favored for the lower $NMHC_s$ case than for the higher $NMHC_s$ case, as more formaldehyde (HCHO) is formed at the lower $NMHC_s$ case through the oxidation by the same amount of OH. Therefore, the increase in the rate of reaction HO_2+NO (R11) is more favored for the lower $NMHC_s$ case than for the higher $NMHC_s$ case under the same condition of NO_x . The enhancement of HO_2 with stratospheric ozone depletion below the low

60 of 69th

clouds is not as much as in the clear sky for the same case of NO_x and $NMHC_s$ in the polluted region.

43.3 Effect of tropospheric pollution

The combined effect of tropospheric pollutants, i.e., O_3 , SO_2 and aerosols (Scenario PASO), on the rates of selected chemical reactions through the radiation changes are shown in Figure 27 for the polluted continent. The reactions $O(^1D)+H_2O$ (R2) and HO_2+NO (R11) are still most sensitive to the perturbations, which occurs mainly in the lower troposphere. The decrease in the rate of reaction HO_2+NO (R11) is mainly due to the aerosols, which predominates over that of reaction $O(^1D)+H_2O$ (R2) in the lower boundary layer. The decrease in the rate of reaction $O(^1D)+H_2O$ (R2) due to O_3 and SO_2 as well as the aerosols is significant in the upper boundary layer and the lower free troposphere and predominates over that of reaction HO_2+NO (R11) there.

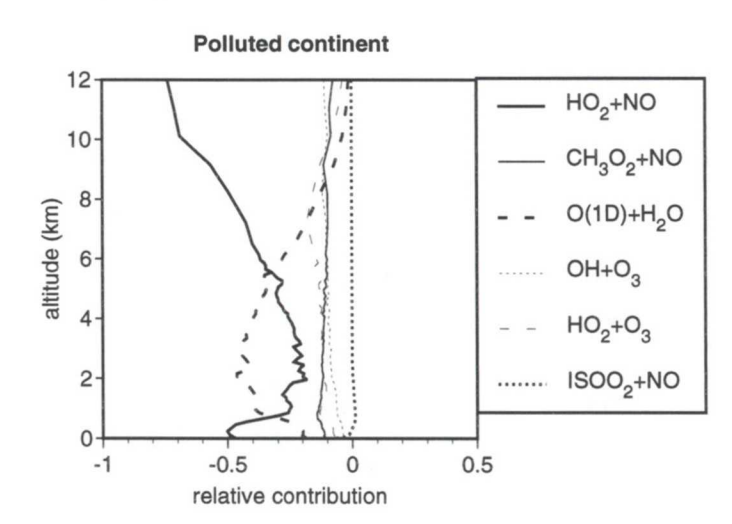


Figure 27 The relative contributions of important chemical reactions to the variation in the net production of ozone, $\Delta rate_i / \sum |\Delta rate_i|$, due to tropospheric pollution through radiation variations (PASO) with respect to the clear-sky condition (REF0).

TNO-MEP - R 96/406 61 of 69th

5. Conclusions

The extended PHATIMA has been used to study the effects of clouds, stratospheric ozone depletion, and tropospheric pollution on the chemical budget of ozone in the troposphere over the ocean, the clean continent and the polluted continent through the changes in photolysis rates. The photodissociation rate coefficient of nitrogen dioxide (J_NO_2) and the effective photodissociation rate coefficient of ozone $(J_O_3(^1D)_{\text{eff}})$ are the most important for the perturbations among those of other species in the troposphere. $J_O_3(^1D)_{\text{eff}}$ which includes altered water vapor concentrations as well, is a parameter more useful than $J_O_3(^1D)$ itself for the study of the chemical budget of ozone in the troposphere. The reaction $O(^1D)+H_2O$ (R2) and HO_2+NO (R11) play a dominant role in the responses of the ozone destruction and the ozone production, respectively. The change in the rate of reaction $O(^1D)+H_2O$ (R2) is exclusively caused by the variation in $J_O_3(^1D)_{\text{eff}}$. The change in the rate of reaction HO_2+NO can be due to the variation in J_NO_2 , which converts more NO_2 back to NO_3 and/or due to the variation in $J_O_3(^1D)_{\text{eff}}$, which produces OH and then leads to the formation of HO_2 by the followed reactions.

The reaction $O(^1D)+H_2O$ (R2) and HO_2+NO (R11) are the most important reactions for the response to the perturbation of the clouds, since both J_NO_2 and $J_NO_3(^1D)_{eff}$ change with the clouds. The effect of the thin middle cloud (CDM1: τ =2 at 4-4.5 km) on the net production of ozone is small for all cases. With the thick middle cloud (CDM2: τ =10 at 4-4.5 km), the net production of ozone increases sligtly in both the boundary layer and the free troposphere of the ocean and in the free troposphere of the clean continent, but decreases in the boundary layer of the polluted continent. With the low clouds (CDL1 and CDL2: at 1-1.5 km), the net production of ozone increases in the free troposphere of all regions, but decreases in the boundary layer of the clean and polluted continents.

The reaction $O(^1D)+H_2O(R2)$ is the most important reaction for the response to the perturbation of stratospheric ozone depletion, since the response of $J_O_3(^1D)_{\text{reff}}$ is most sensitive among those of other species while the response of J_NO_2 is negligible. In the upper free troposphere, the net production of ozone changes slightly with stratospheric ozone depletion due to the low concentration of water vapor there. In the lower troposphere where the water is high, the increase in the rate of reaction $O(^1D)+H_2O(R2)$ leads to the decrease in the net production of ozone over almost all regions, except for the lower boundary layer of the polluted continent. In the polluted boundary layer where the NO_x is high, the increase in the rate of reaction $HO_2+NO(R11)$, due to the enhancement of HO_2 , is also important and may be larger than that of reaction $O(^1D)+H_2O(R2)$, leading to the increase in the net production of ozone in the lower boundary layer of the polluted continent.

The enhancement of HO₂ is more favored for the lower NMHC_s case than for the higher NMHC_s case, as more formaldehyde (HCHO) is formed at the lower

 $NMHC_s$ case through the oxidation by the same amount of OH. Therefore, the increase in the rate of reaction HO_2+NO (R11) is more favored for the lower $NMHC_s$ case than for the higher $NMHC_s$ case under the same condition of NO_x . That is why the response of the net production of ozone to stratospheric ozone depletion is not only determined dominately by the NO_x , but also affected secondly by the $NMHC_s$. In the polluted boundary layer, the increase in the net production of ozone is more favored in the $NMHC_s$ limited region, and less or not favored in the NO_x limited region.

The effect of tropospheric pollution on the net production of ozone through changes in radiation by ozone (O_3) , sulfur dioxide (SO_2) and aerosols occurs mostly in the lower troposphere, which can offset the effect of stratospheric ozone depletion in the polluted boundary layer. The reactions $O(^1D)+H_2O$ (R2) and HO_2+NO (R11) are still most sensitive to the perturbations. The decrease in the rate of reaction HO_2+NO (R11) is mainly due to the aerosols, which predominates over that of reaction $O(^1D)+H_2O$ (R2) in the lower boundary layer. The decrease in the rate of reaction $O(^1D)+H_2O$ (R2) due to O_3 and SO_2 as well as the aerosols predominates over that of reaction HO_2+NO (R11) in the upper boundary layer. Among the pollutants of this study, the effect of the aerosols is most significant while the role of SO_2 is very small.

Above all, the effects of clouds, stratospheric ozone depletion, and tropospheric pollution on the chemical budget of ozone in the troposphere through the changes in photolysis rates have been evaluated for the oceanic, clean continental and polluted continental regions. The chemical coherent characteristic represented by the distributions of trace gases, such as NO_x, CO, NMHC_s, and O₃, has been assumed for each region, respectively. In pratice, the distributions of these trace gases are generally varied even for the same region, the polluted continent in particular. Therefore, the results of this study can be considered only for a typical situation. In addition, the profile of water vapor from a specific site is adopted for the continent in the model, which can be quite different at other sites. Due to the varied distribution of trace gases, NO_x and water vapor in particular, photochemical modelling based on the analysis of field observations is needed to examine the ozone budget over a specific region. For the three-dimensional model simulations, the calculated chemical budget of ozone can be influenced not only by the estimated source distribution of ozone precursors, but also by the prognostic climatological distribution of water vapor.

TNO-MEP - R 96/406 63 of 69th

6. References

Chameides, W.L., and J.C.G. Walker, A photochemical theory of tropospheric ozone, J. Geophys. Res., 78, 8751-8760, 1973.

Chin, M., D.J. Jacob, J.W. Munger, D.D. Parrish, B.G. Doddridge, Relationship of ozone and carbon monoxide over North America, J. Geophys. Res., 99, 14,565-14,573, 1994.

Crutzen, P.J., Photochemical reactions initiated by and influencing ozone in unpolluted tropospheric air, Tellus, 26, 47-57, 1974.

Davis, D.D., J. Crawford, G. Glen, W. Chameides, S. Liu, J. Bradshaw, S. Sandholm, G. Sachse, G. Gregory, B. Anderson, J. Barrick, A. Bachmeier, J. Collins, E. Browell, D. Blake. S. Rowland, Y. Kondo, H. Singh, R. Talbot, B. Heikes, J. Merrill, J. Rodriguez, R. Newill, Assessment of ozone photochemistry in the Western North Pacific as inferrred from PEM-West A observation during the fall 1991, J. Geophys. Res., 101, 2111–2134, 1996

Fishman, J., V. Ramanathan, P.J. Crutzen, and S.C. Liu, Tropospheric ozone and climate, Nature, 282, 818-820, 1979.

Flatφy, F., Φ. Hov, and H. Smit, 3D model studies of exchange process of ozone in the troposphere over Europe, J. Geophys. Res., 100, 11,465-11,481, 1995.

Fuglestvedt, J.S., J.E. Jonson, and I.S.A. Isaksen, Effects of reduction in stratospheric ozone on tropospheric chemistry through changes in photolysis rates, Tellus, 46B, 172-192, 1994.

Intergovernmental Panel on Climate Change (IPCC), Climate change, Report by Working Group 1, Cambridge University Press, Cambridge, 1990.

Jacob, D.J., J.A. Logan, R.M. Yevich, G. M. Gardner, C. M. Spivakovsky, S.C. Wofsy, J.W. Munger, S. Sillman, M.J. Prather, M.O. Rodgers, H. Westberg, and P.R. Zimmerman, Simulation of summertime ozone over North America, J. Geophys. Res., 98, 14,797-14,816, 1993a.

Jacob, D.J., J.A. Logan, G. M. Gardner, R.M. Yevich, C. M. Spivakovsky, S.C. Wofsy, Factors regulating ozone over the United States and its export to the global atmosphere, J. Geophys. Res., 98, 14,817-14,826, 1993b.

Junge, C.E., Global ozone budget and exchange between stratosphere and troposphere, Tellus, 14, 363-377, 1962.

Kanakidou, M., and P.J. Crutzen, Scale problems in global tropospheric chemistry modelling: Comparison of results obtained with a three-dimensional model, adopting longitudinally uniform and varying emissions of NO_x and NMHC, Chemosphere 26 787-801, 1993.

Lacis, A.A., D.J. Wuebbles, and J.A. Logan, Radiative forcing of climate by changes in the vertical distribution of ozone, J. Geophys. Res., 95, 9971-9981, 1990.

Law, K.S., and J.A. Pyle, Modelling trace gas budgets in the troposphere, 1. ozone and odd nitrogen, J. Geophys. Res., 98, 18,377-18,400, 1993.

Lelieveld, J., and P.J. Crutzen, Role of deep cloud convection in the ozone budget of the troposphere, Science, 264, 1759-1761, 1994.

Lelieveld, J., and R. Van Dorland, Ozone chemistry changes in the troposphere and consequent radiative forcing of climate, in Atmospheric Ozone as a Climate Gas, edited by W.C. Wang and I.S.A. Isaksen, pp. 227-258, Springer-Verlag, New York, 1995.

Levy, H., II, Normal atmosphere: Large radical and formaldehyde concentrations predicted, Science, 173, 141-143, 1971.

Lin, X., M. Trainer, S.C. Liu, On the non-linearity of the tropospheric ozone production, J. Geophys. Res., 12, 15,879-15,888, 1988.

Liu, S.C., D. Kley, M. Mcfarland, J.D., Mahlman, and H. Levy II, On the origin of tropospheric ozone, J. Geophys. Res., 85, 7546-7552, 1980.

Liu, S.C., M. Trainer, F.C. Fehsendeld, D.D. Parrish, E.J. Williams, D.W. Fahey, G. Hübler, and P.C. Murphy, Ozone production in the rural troposphere and the implications for regional and global ozone distributions, J. Geophys. Res., 92, 4191-4207, 1987.

Liu, S.C., and M. Trainer, Response of the tropospheric ozone and odd hydrogen radicals to column ozone change, J. Atmos. Chem., 6, 221-233, 1988.

Liu, S.C., Model studies of background ozone formation, in Tropospheric Ozone, edited by I.S.A. Isaksen, pp. 303-318, NATO ASI Series, D. Reidel Publishing Company, 1988.

Ma, J., Stratospheric ozone depletion and its effect on tropospheric ozone, Ph.D thesis, Center for Environmental Sciences, Peking University, China, 1992.

TNO-MEP - R 96/406 65 of 69th

Ma, J., Effects of stratospheric ozone depletion on tropospheric chemistry through changes in UV-B radiation, TNO-report, TNO-MW-R 95/127, Delft, The Netherlands, 1995.

Ma, J., Description of the extension of PHATIMA-model, TNO-report, TNO-MEP-R 96/390, Apeldoorn, The Netherlands, 1996.

Madronich, S., Photodissociation in the atmosphere: 1. Actinic flux and the effects of ground reflections and clouds, J. Geophys. Res., 92, 9740-9752, 1987.

Madronich, S., The atmosphere and UV-B radiation at ground level, in Environmental UV Photobiology, edited by A.R. Young et al., pp. 1-39, Plenum Press, New York, 1993.

Matthijsen, J., Modelling of tropospheric ozone and clouds, Ph.D thesis, Utrecht University, Utrecht, The Netherlands, 1995.

McClatchey, R.A., R.W. Fenn, J.E.A. Selby, F.E. Volz, and J.S. Garing, Optical Properties of the Atmosphere, 3rd ed., Tech. Rept. AFCRL-72-0497, Air Force Cambridge Res. Labs., Bedford, Massachusetts, 1972.

McKeen, S.A., D. Kley, and A. Volz, The historical trend of tropospheric ozone over western Europe: a model perspective, proc,. 4th quadrennial ozone symposium 1988, R.D. Bojkov and P. Fabian (eds.), Ozone in the atmosphere, 1989.

Meijer, E.W., J.M. Matthijsen, M.G.M. Roemer, Phatima 1D-model: Photochemistry and transport in mid-latitudinal atmosphere, MW-TNO report R 94/20, Delft, The Netherlands, 1994.

Müller, J.-F., and Guy Brasseur, IMAGES: A three-dimensional chemical transport model of the global troposphere, J. Geophys. Res., 100, 16,445-16,490, 1995.

Parrish, D.D., D.W. Fahey, E.J. Williams, S.C. Liu, M. Trainer, P.C. Murphy, D.L. Albritton, and F.C. Fehsenfeld, Background ozone and anthropogenic ozone enhancement at Niwot Ridge, Colorado, J. Atmos. Chem., 4, 63-80, 1986.

Pickering, K.E., A.M. Thompson, R.R. Dickenson, W.T. Luke, D.P. McNamara, J.P. Greenberg, and P.R. Zimmerman, Model calculations of tropospheric ozone production potential following observed convective events, J. Geophys. Res., 95, 14,049-14,062, 1990.

Ramanathan, V., L. Callis, R. Cess, J. Hansen, I. Isaksen, W. Kuhn, A. Lacis, F. Luther, J. Mahlman, R. Reck, and M. Schlesinger, Climate-chemical interactions and effects of changing atmospheric trace gases, Rev. Geophys., 25, 1441-1482, 1987.

Roelofs, G.J., and J. Lelieveld, Distribution and budget of O_3 in the troposphere calculated with a chemistry general circulation model, J. Geophys. Res., 100, 20,983-20,998, 1995.

Roemer, M.G.M., Ozone and the greenhouse effect, IMW-TNO report R 91/227, Delft, The Netherlands, 1991.

Roemer, M.G.M., and K.D. van den Hout, Emissions of NMHCs and NO_x and global ozone production, in Proceedings of the 19th NATO/CCMS International Technical Meeting on Air Pollution Modelling and Its Application, North Atlantic Treaty Organization/Committee on the Challenges of Modern society, (eds.: van Dop and Kallos), September 29-October 4, 1991, Grete, Greece, Plenum Press, New York, 1992.

Roemer, M., The tropospheric budgets and trends of methane, carbon monoxide and ozone on a global scale, MEP-TNO report R 95/207, Delft, The Netherlands, 1995.

Roemer, M., M. Boersen, P. Builtjes, and P. Esser, Budgets of ozone on a global and regional scale, MW-TNO report P 95/039, Delft, The Netherlands, 1995.

Schnell, R.C., S.C. Liu, S.J. Oltmans, R.S. Stone, D.J. Hoffman, E.G. Dutton, T. Deshler, W.T. Sturges, J.W. Harder, S.D. Sewell, M. Trainer, and J.M. Harris, Decrease of summer tropospheric ozone concentrations in Antarctica, Nature, 351, 726-729, 1991.

Simpson, D., Photochemical model calculations over Europe for two extended summer periods: 1985 and 1989, Model results and comparison with observations, Atmos. Environ., 27A, 921-943, 1993.

Strand, A., and Ø. Hov, A two-dimensional global study of tropospheric ozone production, Geophys. Res., 99, 22,877-22,895, 1994.

Thompson, A.M., and R.J. Cicerone, Clouds and wet removal as causes of variability in the trace-gas composition of the marine troposphere, J. Geophys. Res., 87, 8811-8826, 1982.

Thompson, A.M., The effect of clouds on photolysis rates and ozone formation in the unpolluted troposphere, J. Geophys. Res., 1341-1340, 89, 1984.

Thompson, A.M., and R.J. Cicerone, Possible perturbations to atmospheric CO, CH4, and OH, J. Geophys. Res., 91, 10,853-10,864, 1986.

TNO-report

TNO-MEP - R 96/406 67 of 69th

Thompson, A.M., R.W. Stewart, M.A. Owens, and J.A. Herwehe, Sensitivity of tropospheric oxidants to global chemical and climate change, Atmos. Environ., 23, 519-532, 1989.

Thompson, A.M., and R.W. Stewart, Effect of chemical kinetics uncertainties on calculated constituents in a tropospheric photochemical model, J. Geophys. Res., 96, 13,089-13,108, 1991.

Trainer, M., E.Y. Hsie, S.A. McKeen, R. Tallamraju, D.D Parrish, F.C. Fehsenfeld, and S.C. Liu, Impact of natural hydrocarbons on hydroxyl and peroxy radicals at a remote site, J. Geophys. Res., 92, 11,879-11,894, 1987.

Trainer, M., M.P. Buhr, C.M. Curran, F.C. Fehsenfeld, E.Y. Hsie, S.C. Liu, R.B. Norton, D.D. Parrish, and E.J. Williams, Observations and modelling of the reactive nitrogen photochemistry at a rural site, J. Geophys. Res., 96, 3045-3063, 1991.

Van den Hout, K.D. van den, M.G.M. Roemer, and P.J.H. Builtjes, NO_x in the global troposphere: Emissions, concentrations and model calculations, MT-TNO report R 90/223, Delft, The Netherlands, 1990.

Van Weele, M., and P.G. Duynkerke, Effect of clouds on the photodissociation of NO₂: Observations and modelling, J. Atmos. Chem., 16, 231-255, 1993.

Van Weele, M., Effect of clouds on ultraviolet radiation, Ph.D thesis, Utrecht University, Utrecht, The Netherlands, 1996.

Weinstock, B., and H. Niki, Carbon-monoxide balance in nature, Science, 176, 290-292, 1972.

Wofsy, S., J.C. McConell, and M.B. McElory, Atmospheric CH4, CO, and CO2, J. Geophys. Res., 77, 4477-4495, 1972.

World Meteorological Organization (WMO), Scientific Assessment of Stratospheric Ozone: 1989, Global Ozone Research and Monitoring Project, Rep. 20, Geneva, Switzerland, 1990.

World Meteorological Organization (WMO), Scientific Assessment of Ozone Depletion: 1991, Global Ozone Research and Monitoring Project, Rep. 25, Geneva, Switzerland, 1992.

World Meteorological Organization (WMO), Scientific Assessment of Ozone Depletion: 1994, Global Ozone Research and Monitoring Project, Rep. 37, Geneva, Switzerland, 1995.

TNO-MEP - R 96/406 69 of 69th

7. Authentication

Name and address of the principal: Institute for Marine and Atmospheric Research (IMAU) Utrecht University Utrecht

Names and functions of the cooperators:

R. Guicherit

M.G.M. Roemer

M. van Weele (IMAU)

Names and establishments to which part of the research was put out to contract:

Date upon which, or period in which, the research took place:

1995 - 1996

Signature:

Approved by:

J. Ma

Research Co-ordinator

H. P. Baars

Head of the Department of

Environmental Quality

Date: 18-12-1996

Date: 1/11/96